A STUDY OF CHARGE INJECTION IN

ITO/PEDOT/MEH-PPV/Ca/Al PLEDs

AND

LIFT-OFF PROCESS IN POSITIVE PHOTO RESIST

A Thesis Submitted

In

Partial Fulfillment of the Requirements
For the Degree of

Master of Technology

By

TALARI MANOJAYA
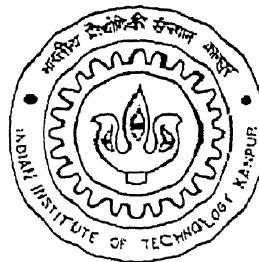
To the
DEPARTMENT OF ELECTRICAL ENGINEERING
INDIAN INSTITUTE OF TECHNOLOGY, KANPUR

AUGUST, 2005

CERTIFICATE

This is to certify that the work contained in the thesis entitled "A STUDY OF CHARGE INJECTION IN ITO/PEDOT/MEH-PPV/Ca/Al PLEDs AND LIFT-OFF PROCESS IN POSITIVE PHOTO RESIST" by Talari Manojaya (Roll No. Y3104102) has been done under our supervision and this work has not been submitted elsewhere for a degree.
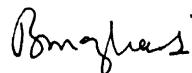

Dr. Baquer Mazhari
Associate Professor

Dr. Jitendra Narain
Chief Research Engineer

Department of Electrical Engineering
Indian Institute of Technology
Kanpur-208016

POST GRADUATE OFFICE
THESIS SUBMITTED ON 4|8|05
I.I.T., KANPUR-208 016

2nd AUGUST 2005

Acknowledgement

ABSTRACT

To meet the challenges of the PLED technology, we have made an attempt to find the nature of currents in the ITO/PEDOT/MEH-PPV/Ca/Al device. Hole only devices are fabricated to observe the dependence of hole current on the thickness of the injection layer in the device with gold as cathode. A similar study has been done for electron only device with magnesium as anode. Both the studies provide the necessary information to design a device having a better charge balance which ultimately leads to improvement in efficiency. We had also made an attempt to optimize Lift-Off:- Image reversal process with positive photoresist for display application.

Dedicated To

My Father

(Shri Narsimlu Talari)

Contents

PART:-I

PART:-II

List of Figures

Abbreviations and Symbols -1

HOMO	Highest Occupied Molecular Orbit
LUMO	Lowest Unoccupied Molecular Orbit
LCD	Liquid Crystal Display
TFT	Thin Film Transistor
TV	Television
PC	Personal Computer
OLED	Organic Light Emitting Diode
PLED	Polymer Light Emitting Diode
RCA	Radio Corporation of America
SCLC	Space Charge Limited Current
FN	Fowler-Nordheim
ITO	Indium Tin Oxide
PEDOT	Poly(3,4-ethylenedioxythiophene)
PSS	Poly(StyreneSulfonate)
MEH-PPV	poly[2-methoxy-5-(2'-ethyl-hexyloxy)-1,4-phenylene vinylene]
PPV	Poly (Phenylene Vinylene)
Au	Gold
Mg	Magnesium
Nd	Neodymium
Ca	Calcium
Al	Aluminum
SiO_2	Silicon dioxide
HCL	Hydrochloric acid

HNO$_3$	Nitric acid
NH$_4$OH	Sulfuric acid
Si	Silicon
DI	De Ionized Water
NH$_4$OH	Ammonium Hydroxide
H$_2$O$_2$	Hydrogen Peroxide
PPR	Positive Photo Resist
PAC	Photo Active Compound
IR	Image Reversal
VLSI	Very Large Scale Integration
UV	Ultra Violet
PR	Photo Resist
PANI	Poly Aniline
DUT	Device Under Test

PHYSICAL CONSTANTS

Constant	Symbol	SI Units	Other Units and/or Comments
Electron volt	eV	1.602×10^{-19} J	---
Electron mass	m_e	9.110×10^{-31} kg	511.1 KV/c^2
Proton mass	m_p	1.673×10^{-27} kg	938.3 MeV/c^2
Neutron mass	m_n	1.674×10^{-27} kg	939.6 MeV/c^2
Unified mass unit	u	1.661×10^{-27} kg	931.5 MeV/c^2
Elementary charge	e	1.602×10^{-19} C	---
Planck's constant	h	6.626×10^{-34} J·s	4.136×10^{-15} eV·s
Planck's constant $/(2\pi)$	$h/2\pi$	1.054×10^{-34} J·s	6.582×10^{-16} eV·s
Planck's constant · c	$h·c$	---	1240 eV·nm
Planck's constant	h	6.626×10^{-34} J·s	4.136×10^{-15} eV·s
pi	π	3.142	---
Coulomb's law constant	$1/(4\pi\varepsilon_o)$	8.988×10^9 N·m^2/C^2	9×10^9 N·m^2/C^2
Brightness	nits	Cd/m^2	
Angstrom	A^0	10^{-10} m	10^{-8} cm

INTRODUCTION

1.1   Review

As new horizons are opening up, the advent of organic electronics has already caused a stir in science and technology. It is an exciting time for engineers to look into the minute issues of the technology and explore the new possibilities of organic electronics. OLED technology offers a low cost thin film large area option that exploits electroluminescence and uses material as cheap as plastic or glass. Polymer devices typically begin to generate light at 2-3 volts.

While LCDs are passive devices, active matrix LCD displays controlled by an array of TFTs provide heightened color and brightness. But they require back lighting which accounts for about half of their power requirements. This is where the PLED or OLED devices made by placing a series of organic thin film between electrodes (conductors) scores big. When an electric current is applied a process called electroluminescence emits a bright light. Since these are self-luminous they save on the power required for backlighting. This makes it suitable for a wide range of applications from TV and advertising displays to tiny mobile phones or pocket PC screens.
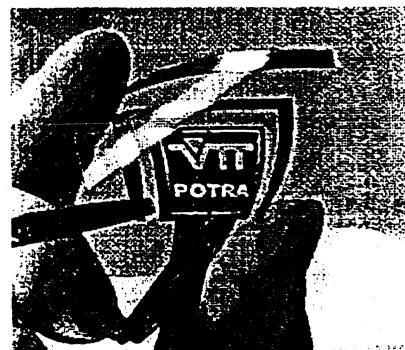
Fig 1.1: Shows Displays made of LCDs (Laptop) and OLED (flexible Plastic)

The viewing angle of LCDs is less compared to OLEDs. Hence the properties of OLEDs are being exploited by display makers.

1.2   Brief historical overview of Electroluminescence Diodes:

The first report pertaining to electroluminescence of an organic semiconductor by Pope *et al.* goes back to 1963. They observed luminescence from single crystalline anthracene with a few tens of microns thick using silver electrodes and voltages being hundred volts with an efficiency of nearly 1%. The difficulties with respect to crystal growth and the large voltages required for light emission, limited the practical application of OLEDs. Tang *et al.* in 1987, revived the interest in organic EL by using evaporated thin amorphous films of nearly 100 nm as emissive layer, which reduced the operating voltages significantly to less than 10 V [3]. The first publication describing electroluminescence from a polymer is by Burroughness in 1990.

Furthermore, the LED performance was greatly improved, by means of additional charge-transport layers. Double-layer LEDs with high peak brightness and internal electroluminescence efficiencies up to 4% have been reported. The long-term device stability and device efficiencies of polymer LEDs are rapidly increasing, but improvements are still desired. Polymer LEDs currently has less device lifetime because of degradation. Another problem is the interface and contact stability, as low work function metals oxidize in the presence of either H_2O or O_2. The temperature stability is an important parameter for display applications, displays must withstand fairly wide range in temperature.

1.3 Conjugated polymers as semiconducting materials

Conjugated polymers attract much interest currently, for use as active component in optoelectronic applications, viz. light-emitting diodes, photodiodes, photovoltaic cells, thin film transistors etc. They have a backbone consisting of alternating single and -- double bonds (figure 1.1). In Conjugated polymers, electrons are delocalized throughout the entire polymer and are free to move. The overlap of π bonding and π^* antibonding molecular orbitals forms a continuous system of electron density along the backbone. Conjugated polymers have bandgaps in the range of 1 to 4 eV, allowing stable optical excitations and mobile charge carriers. The extent of this overlap (conjugation length) together with the bond alternation determines the HOMO-LUMO (frontier orbits) band gap.
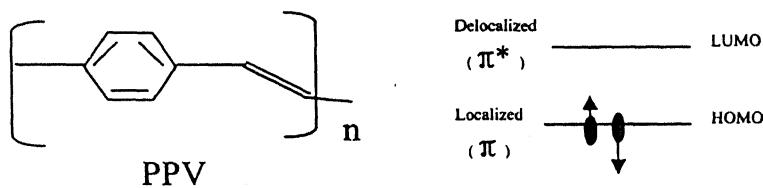
Fig 1.2: Polymer with alternative single and double bond and the energy level in ground state.

These materials are often strongly fluorescent and emit in the range from near infrared to the ultraviolet. Especially PPV and soluble derivatives thereof, are of great interest, due to the emission in the visible region and high luminescence quantum yields. The wavelength of emission depends on the extent of conjugation/delocalization, and can be controlled by modification of the chemical structure. This can be done by the attachment of additional functional groups, which alter the electronic structure of the conjugated polymer. So, light emission is possible by radiative recombination from singlet excitons from the HOMO-LUMO energy gap of the polymer covering the entire spectrum.

1.4 Excitations in organic semiconductors

Normally, semiconductor material will be in its ground state. To transport charge, and/or emit light, the semiconductor needs excitation, and in the case of charge transport, these excitations also need to be mobile.

1.4(a) Polarons and excitons

When an electron is taken away from the HOMO or added to the LUMO of a molecule, the resulting molecule is termed a radical ion, namely a radical cation for positive charge, and radical anion for negative charge. After removal or addition of the electron, molecular orbitals and the positions of nuclei will respond by a relaxation to a new position of minimum energy. These radical ions are often called **polarons**, (electron / hole polaron, respectively). Due to the strong coupling between the charge carrier and the local lattice relaxation, removing an electron looses some energy than the HOMO called **Ionization potential Ip,** and an electron joining the molecule gains some energy than the LUMO is called **Electron affinity** χ.
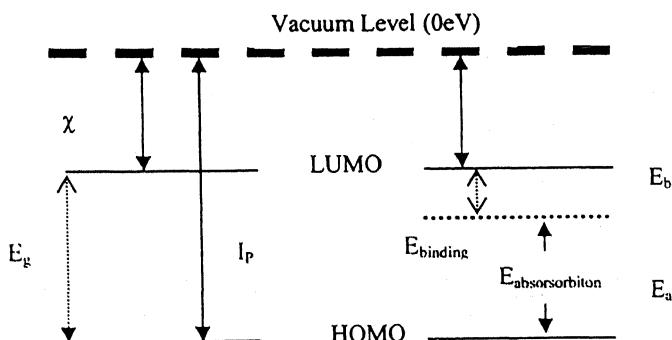
Fig 1.3: Energy band diagram with frontier orbits, where χ is electron affinity, E_g is the bandgap, I_P is the Ionization potential
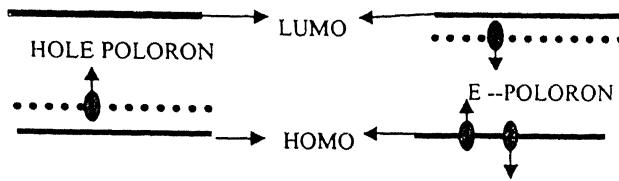
Fig 1.4: Shows two different types of polarons:- hole poloran and electron poloran when excitated

Apart from polarons, the most important excitation in an organic semiconductor is **exciton**. This can be visualized as an electron that is removed from the HOMO, but is positioned into the LUMO instead of being removed entirely. A typical way of transfer of an electron from the HOMO into the LUMO is via the absorption of a photon (shining light). This exciton is electrically neutral. Alternatively, an exciton can result from the combination of a hole and an electron polaron. Due to the mutual attraction of electron and hole in the exciton, and structural relaxation of the molecule, the energy difference between the excitonic state and the ground state is lower than the difference between Ip and Ea, which in turn is lower than the difference between HOMO and LUMO. This energy difference is known as **exciton binding energy** Eb.
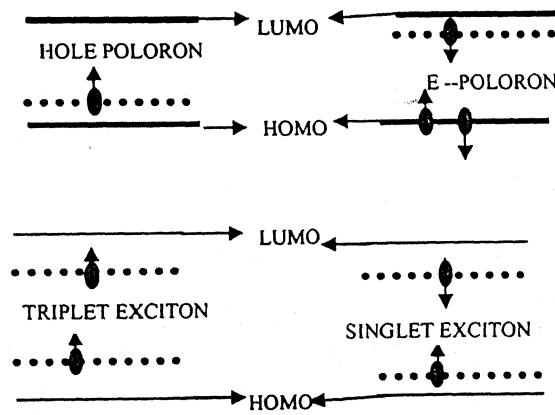
Fig 1.5: Excitations in Organic semiconductors showing the singlet and triplet exciton, Singlet excition gives light while triplets wont.

There are three ways in which hole and electron spin can combine so that the resulting overall spin part of the wave function is symmetric under particle exchange, and has total spin S = 1:- namely $< \uparrow\uparrow >$, $< \downarrow\downarrow >$, and $1/\sqrt{2}$ ($< \uparrow\downarrow >$ + $< \downarrow\uparrow >$).

These excitons are called **triplet excitons.** The decay of Triplet exciton is a non-radiative process which does not give any light. Another part of spins of the wave function that is antisymmetic under particle exchange is, namely $1/\sqrt{2}$ ($< \uparrow\downarrow >$ - $< \downarrow\uparrow >$), and total spin S = 0 is called a **singlet exciton.** The decay of singlet exciton may be a radiative process which gives light.

1.5   Summary:

Understanding transport in polymer light-emitting diodes (PLEDs) has been complicated by the presence of both electrons and holes in working devices for which complete analytical models do not exist. The charge injection plays an important role in the device performance, because device efficiency depends on how many photons are generated in the emissive layer. The transport of these charges depends on the mobility, electric fields and temperature.

To meet the challenges of this growing technology we have to be conversant with the fabrication and characterization aspects of the PLEDs. So far, no adequate description of the J-E behavior of Polymer LEDs has been provided. In the present study, we provide consistent description of the J-V characteristics of MEH-PPV devices. Polymer light emitting diodes (PLEDs) charge injection, which is an important criterion in PLEDs, is studied by identifying injection current density for electrons and holes separately. By studying these current densities separately we can create charge balance. Using ITO/PEDOT for hole injection and Ca/Al for electron injection layers we find that the J-E characteristics are dominated by bulk-conduction properties of MEH-PPV at fields 10^5-10^6 V/cm.

1.6   Thesis Layout:

In Chapter-2, the different mechanisms of charge injection and charge transport are studied. In Chapter-3, a number of experiments have been performed on hole only device by varying PEDOT on ITO/PEDOT/MEH-PPV/Au PLED. In this device with the nature of hole current, the role of PEDOT on interface roughness and yield is studied. Chapter-4, numerous experiments have been performed similar to chapter 3 for the nature of electron current by varying calcium thickness in the Mg/MEH-PPV/Ca/Al PLEDs device. In addition single layer devices have been fabricated to study the nature of electron current. We have also calculated electron current by fabricating a ITO/PEDOT/MEH-PPV/Ca/Al PLED and the total current in such a device is due to electron and hole current, once the quantity of hole current is known, then the electron current can also be calculated with simple a subtracting of hole current from total current. Finally, Chapter 5 concludes the thesis with an interesting topic on 'lift-off' process with positive photo resist process, in this chapter the utility of ribs for the cathode isolation on OLEDs is studied. And followed by the summary, results, and future work.

CHAPTER – II

Physics of Charge injection and Charge Transport

2.1   General Introduction of OLED

PLED/OLED is an electronic device that emits light when a potential is applied to the electrodes. A fluorescent polymer is sandwiched between the anode and the cathode. The anode is typically Indium-Tin Oxide (ITO), which is transparent and allows light to escape. On top of ITO, an emissive polymer layer is deposited, followed by a layer of Aluminum (Al) which acts as cathode.
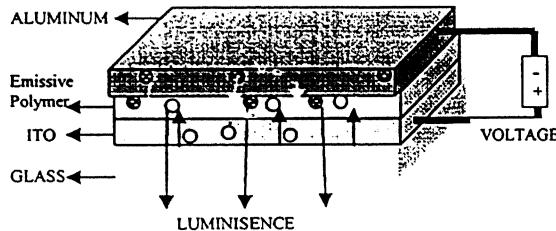
Fig 2.1: (a)
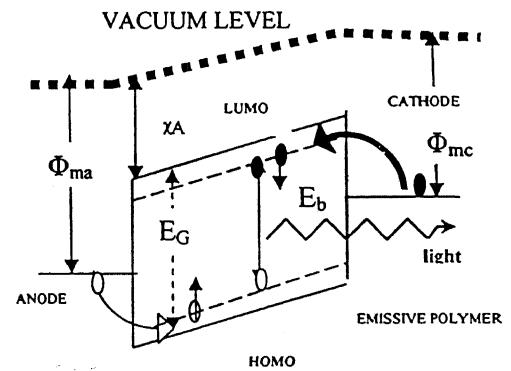
Fig 2.1: (b)

Fig 2.1 :(a) Simple PLED structure ITO/ MEH-PPV /Al

(b) Energy band diagram under the influence of electric field

For a PLED to function, both the holes and electrons are required, from the anode and cathode respectively. The objective of the present chapter is to understand the injection and transport of these charge carriers.

2.2: Interface barrier & Charge Injection

Three different types of contacts are described for a metal – semiconductor (intrinsic) contact.

(I) When ($\Phi_M = \Phi_S$), the Fermi-levels of the metal and the semiconductor are already lined out, and no charge redistribution is required upon contact. This is called a neutral contact as in Fig 2.2(a): both the electron and hole contact have an interfacial concentration of charge equal to their intrinsic free carrier concentration.
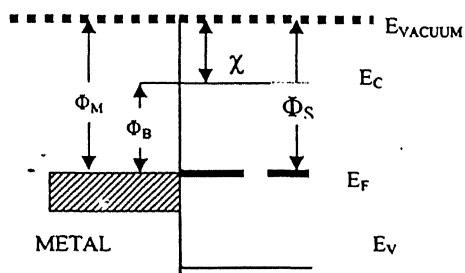
2.2 (a)   SEMICONDUCTOR
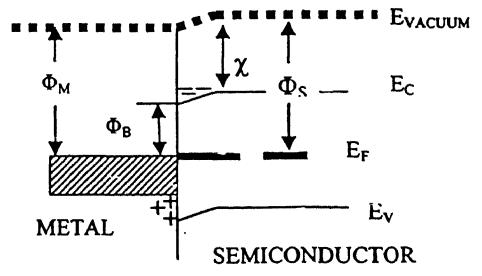
2.2 (b)

Fig 2.2: (a): Barrier for an intrinsic semiconductor for $\Phi_M = \Phi_S$

(b): Barrier for an intrinsic semiconductor for $\Phi_M < \Phi_S$

(II)   When the metal work-function is smaller than the semiconductor work-function (Φ_M Φ_S) as shown in Fig.2.2 (b), the electrons are accumulated in the semiconductor, and the electron contact is ohmic, as electrons move from higher potential to lower potential. The hole contact is now injection limited. where $\Phi_B = \Phi_M - \chi$
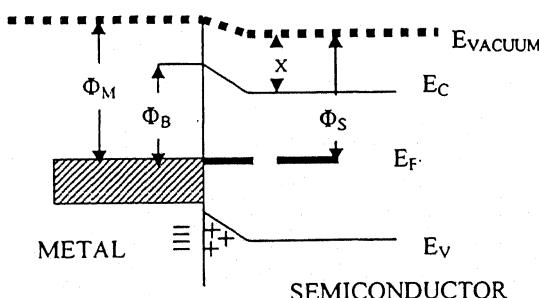
Fig 2.2 (c): Barrier for an intrinsic semiconductor for ($\Phi_M > \Phi_S$)

(III)   When the metal work-function is larger than the semiconductor work-function $(\Phi_M > \Phi_S)$ as shown in Fig.2.2 (c), the electrons are depleted from the semiconductor. Due to the electron-depletion, the contact region cannot supply enough charge carriers to the bulk of the semiconductor, and the contact is called blocking or injection-limited for electrons. At the same time, the contact region contains excess of holes. As a result, the contact region can supply hole charges demanded by the bulk of the semiconductor, and the contact is called ohmic or bulk-limited for holes. Where $\Phi_B = \Phi_M - X$.

The experimental definition of contact barrier type, Ohmic contact for SCLC and injection limited contact for Contact Limited Current is different from the definitions of the Ohmic, neutral and injection limited contacts from the intrinsic semiconductor to organic electronics, because the Fermi level in polymers is not exactly defined.

It is estimated from theoretical calculations that for a contact barrier of $\Phi_B < 0.2\ eV$ the current is space charge limited at room temperature [6] and consequently the contact is Ohmic. When $\Phi_B > 0.2\ eV$, the current that the contact can supply is smaller than SCLC (at room temperature) and the current is limited by injection. As a result, from the experimental definition, the contact is called Injection-limited, irrespective of the fundamental definition, that can be either Ohmic, neutral or injection-limited, depending on $\Phi_M - \Phi_S$.

Charge injection in metal is controlled by the work function only, irrespective of the electron affinity for electron injection and ionization potential for hole injection of the semiconductors.

2.3   Charge transport

In light emitting diodes drift current is combination of both currents, to maximize the efficiency, the hole current should be equal to the electron current. If this is ensured, every hole will get an electron for recombination. But there is no analytical model which

can give necessary information to fabricate such a device. And it is not possible to measure the magnitude of the hole and electron currents in a PLED separately. Therefore, one has to fabricate two kinds of devices, viz. electron only and hole only devices separately such that $J = J_e$, for electron only device and $J = J_h$, in hole only device respectively.

Now if we know the magnitude of the both current and try to optimize the currents in a composite device then the total current should be equal to both the currents. But this may not be true for the real device because the electron current try to influence the hole current and vice versa.

As discussed earlier the currents need to inject into the active layer of the device, one has to know what sort of current is flowing, like ohmic, thermionic or tunneling. To analyse the $J–V$ characteristics, we evaluated the influence of several mechanisms that are usually accounted in polymer devices.

2.3(a):   Ohms Law

In an organic device the total current is given by the drift current only, if the background doping is nil.

$$J_{total} = J_{drift} = J_e + J_h \ ---(1)$$

Where J_e and J_h are the electron current and hole current respectively.

The drift current density is given by the following equations:-

$$J_{drift} = q(n\mu_n + p\mu_p)E \ ---(2)$$
$$or$$
$$J_{drift} = q(n\mu_n + p\mu_p)\frac{V}{L} \ ---(3)$$

q, n, p V, L, μ_p and μ_n are the charge, magnitude of electrons, magnitude of holes, applied voltage, length, hole mobility and electron mobility.

Current density is linearly proportional to the applied electric field. This class of conduction is dominating at low electric fields.

2.3(b)   Space Charge Limited Current:

For conjugated polymers like PPV and its derivates the mobility is field dependent, and the maximum current J_{SCLC} can be found from a numerical calculation. For a field-independent mobility, where no compensation charge is present, the SCLC is directly given by the Mott-Gurney equation (considering the trap free) [5, 6,12].

$$J_{SCLC} = \frac{9}{8} \varepsilon \mu \frac{V^2}{L^3} = \frac{9}{8} \varepsilon_o \varepsilon_r \mu \frac{E^2}{L} \quad ---(4)$$

Where ε_r is the relative permittivity
ε_o is the free space permittivity
E is the electric field across the device
L is the thickness
μ is the common Poole–Frenkel form of the field dependence of the hopping mobility for the free carrier is used [5,6],

$$\mu = \mu_0 \exp \sqrt{(E / E_0)} \quad ---(5)$$

μ_o is the zero-field mobility
E_o the electric-field coefficient to the mobility due to the interaction between charge carriers and randomly distributed permanent dipoles in semiconducting polymers [6].

12

Finally the field dependent space charge current equation is given by

$$J_{SCLC} = \frac{9}{8} \varepsilon_r \varepsilon_o \mu_o \frac{E^2}{L} \exp\left(\gamma\sqrt{E}\right) \quad ---(6)$$

Where γ is the electric field coefficient.

The Log-Log curve gives a better understanding of the characteristics. The slope of the line gives constant value of 2, which specify the Space charge limited current.

$$Slope \; m(V) = \frac{d(Log(J))}{d(Log(V))} \approx 2 \quad ---(7)$$
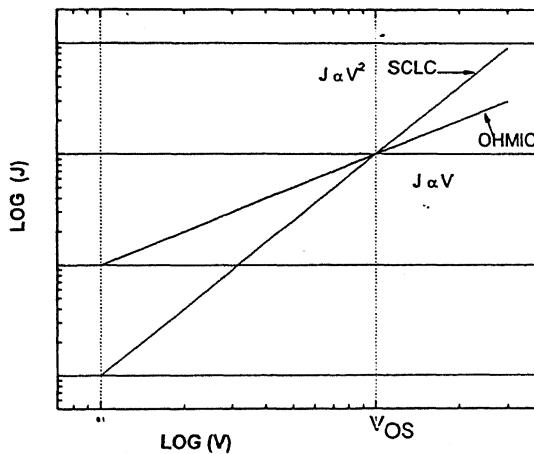
Fig 2.3: Ideal Characteristics of ohmic and space charge limited current.

The slope of the ohmic is 1, and SCLC is 2.

V_{os} is the onset of Space charge limited current

There are two mechanisms for the electron (or hole) transport across a potential barrier: - thermonic emission (i.e. schottky emission) and Field emission (also called FN tunneling).

13

2.3 (c)   Schottky Barrier

At low voltages, when the image force effect is minor, we applied the Schottky barrier model to describe dependence of current J on applied voltage V. Schottky model which assumes a well defined fixed potential barrier at the interface over which the electrons are thermionically emitted [32]. Using this model, with thermionic emission and diffusion of carriers, gives:

$$J = J_S \left(\exp(\frac{qV_{eff} + \Delta\phi}{nk_bT} - 1 \right) - - - (8)$$

$$J_S = A^{**} T^2 \exp\left[-\frac{q\phi_b}{nk_bT} \right] - - - (9)$$

The barrier is lowered in the presence of image-charge effect by an amount $\Delta\Phi$, where Φ_b is the contact barrier potential, V is the applied bias, n is the ideality factor, A^{**} is the effective Richardson constant [19].
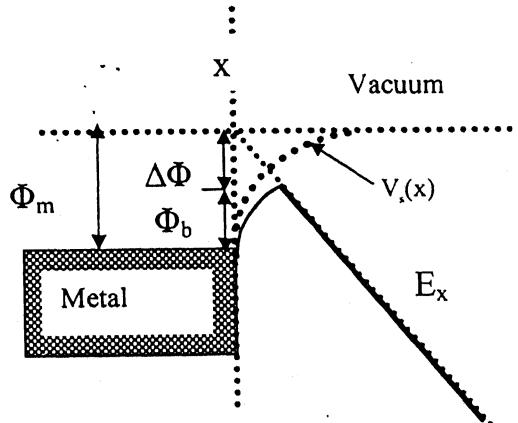
Fig 2.3

Fig 2.4: Energy band diagram with Barrier lowering due to the image force where $V(X)$ is mirror potential at distance x from contact surface (interface)

$$\phi_b = \phi_m - \Delta\phi \quad --- (10)$$

And $\Delta\Phi$ can be calculated by following equation

$$\Delta\phi = \sqrt{\frac{qE(0)}{4\pi\varepsilon_0\varepsilon_r}} \quad --- (11)$$

Φ_b is given by the barrier height lowering due to image force effect.

For a given current density J, equations (6, 7) directly provide the boundary condition for the electric field E (0) at the injecting contact.

2.3(d)   Field Emission:

Field emissions is one of the earliest confirmations of electron tunneling as predicted by the quantum theory in the 1920's by applying a large electric field to a cathode, it makes the electrons tunnel from the cathode through the potential barrier which is modified by the electric field into the vacuum. Field emission theory is conventional experimental method for studying the electronic structure of materials, such as the work function of metal surfaces. The well known Fowler-Nordheim theory gives an analytic dependence of the emission current density on the applied electric field and the work function, by assuming that the emitter is a free-electron-like metal. According to the theory the only controlling quantity that depends on the emission surface is the work-function [9,31].

It is widely used, as simple model for tunneling mechanism from a metals Fermi energy over a barrier into an adjacent material. In this mechanism, the effect of finite

temperature, and the image-force barrier lowering are ignored. Further more, applied voltage is larger the barrier voltage and only tunneling from the metal Fermi energy into the conduction band of semiconductor or insulator (polymer LUMO) are consider[30] , the Fowler-Nordheim equation can be written as:

$$J = \frac{q^3 E^2 m}{8\pi h m^* \phi_b} \exp(-\frac{8\pi\sqrt{2m^*}\,\phi_b^{3/2}}{3hqE}) \quad --(12)$$

Where $J = I/A$;   Where A is the effective contact area; E is the applied electric field Φ_b is the contact barrier height; q, m^*, m, h are the charge, effective mass, free mass and plank constant respectively.

$$E = \frac{V_{eff}}{L} \quad --(13)$$

Where V_{eff} is the applied forward-bias voltage

L is the separation distance between the two electrodes.

Finally, current density is given by

$$J = 1.55 \times 10^{-5} E^2 \phi_b^{-1} \exp(-6.86 \times 10^7 \phi_b^{3/2} E^{-1}) \quad --(14)$$

Where J = current density in *amp/cm²*; E = Electric field at surface in *Volts/cm*

Φ_b =constant barrier height in *Volts*
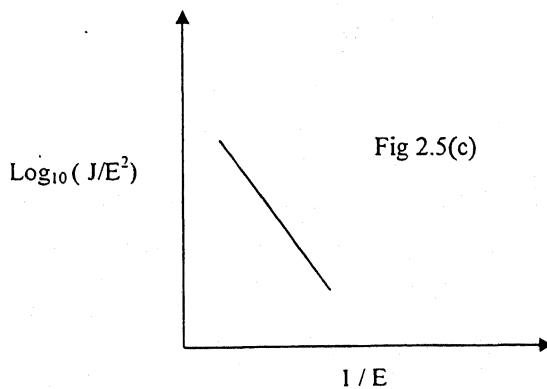
Fig 2.5: Slope from FN-plot gives an indication of effective barrier height

The slope *m(E)* of *Log(J/E²)* versus *(1/E)* plot of the FN- equation will be a negative slope at high electric fields as given below.

$$Slope\ m(E) = \frac{d(\log_{10}^{(J/E^2)})}{d(1/E)} = -2.98 \times 10^7 \phi_b^{3/2} \quad ---(15)$$

or

$$Slope\ m(E) = \frac{d(\log_e^{(J/E^2)})}{d(1/E)} = -6.86 \times 10^7 \phi_b^{3/2} \quad ---(16)$$

An example of FN-plot of equation 15, 16 is shown in Fig 2.4.

Hence we can define Injection current efficiency is the ration of injected current to the SCLC

$$\eta = \frac{Inj\ Ltd}{SCLC}$$

$$\eta = 1\ (SCLC) \qquad ---(17)$$
$$\eta < 1\ (Inj\ Ltd)$$

However the magnitudes of current of Schottky or field emissions (injection limited) are less when compared to the space charge limited current. Hence maximum current in an organic semiconductor is obtained when the injected current is space charge limited current (SCLC).

However, the injection barrier height is not the only parameter that controls the charge transport mode, electric field, charge concentration and mobility are also part of it. At present the general interrelations between these main mechanisms in polymers are established qualitatively; nevertheless, there are still discussions about this in major details.

2.4 QUANTUM EFFICIENCY

The quantum efficiency in PLEDs is affected by the nature of the material used in the emissive polymer and also by the device structure. The electroluminescence efficiency (η_{el}) is defined in equation no.

$$\eta_{el} = \eta_{pl}\, \eta_s\, \eta_i \quad ---(18)$$

Where η_{pl} is the photoluminescence efficiency depends on the emissive material,

η_s is the singlet exciton quantum yield (often taken to be 25%), and

η_i is the charge balance efficiency($\leq$1).

For optimum device performance, the following three factors should be considered:

(1) Carrier injection and transport.

(2) Formation of exciton.

(3) Radiative recombination of exciton.

Thus, it is very important to equalize the number of electrons and holes reaching emissive zone to maximize η_i.
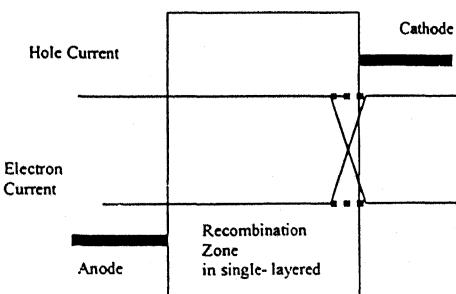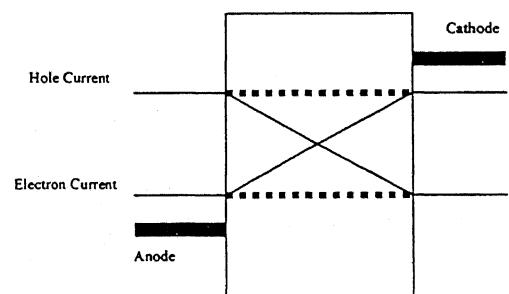
Fig 2.6(a)   Fig 2.6(b)

Fig 2.6 :(a): Recombination Zone in single- layered device unbalanced Charge transport

(b): Balanced Charge transport

18

Holes are highly mobile than electrons in conjugated polymers due to deep traps caused by oxidation electrons which makes them preferentially hole transports [8]. The lower electron mobility results in unbalanced transport and recombination close to the interface of the electron-injecting metal electrode, which causes excition quenching, leading to poor EL efficiencies.

This can be overcome by introducing the same mobility of electron and hole, such that most of the recombination takes place, i.e. current balance $(J_P \approx J_e)$ at present not possible because of the unavailability of suitable materials, or by increasing the length of the polymer thickness so that the recombination does not takes place at the cathode interface, but the operating voltage increases.

2.5   Summary:

The different mechanisms of charge injection and transport have been reviewed. At low electric fields, the current density is linearly proportional to electric field (Voltage) in thermoinic emission. There are two mechanisms for the electron or hole transport across a potential barrier: - thermonic emission (i.e. schottky emission) and Field emission (also called FN tunneling). Thermonic emission is defined for fixed potential barrier at the interface over which the electrons are thermionically emitted. In Field emission, the effect of finite temperature, and the image-force barrier lowering are ignored. Further more, applied voltage is larger the barrier voltage and only tunneling from the metal Fermi energy into the conduction band of semiconductor or insulator (polymer LUMO).

For a field-independent mobility, where no compensation charge is present, the SCLC is used. However the magnitudes of current of these two mechanisms are less when compared to the space charge limited current. Hence maximum current in an organic semiconductor is obtained when the injected current is space charge limited current (SCLC).

CHAPTER – III

HOLE ONLY DEVICE (ITO/PEDOT/MEH-PPV/Au)

3.1   Hole Only Diode Introduction

In order to investigate the hole current in a MEH-PPV device, the electron current needs to be suppressed. As gold has high work function, the Au cathode blocks the injection of electrons into MEH-PPV. In the Fig. 3.1 the energy band diagram of such a device is shown. In forward bias, the hole injection into MEH-PPV from the ITO/PEDOT: PSS electrode is studied. The hole currents are given by space-charge limited current with a field and temperature dependence of the hole mobility [5] and field emission current are given in Parker [4].
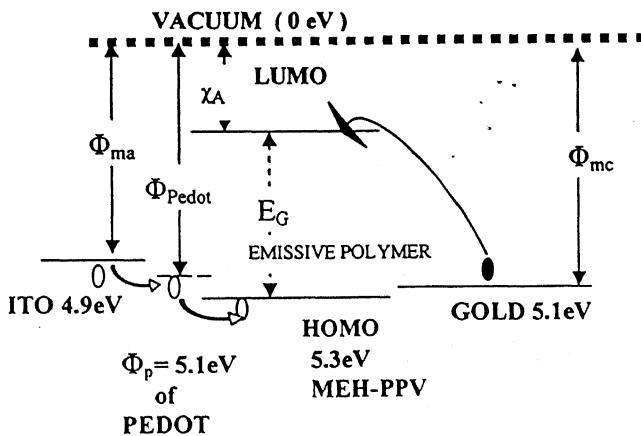
Fig 3.1: Energy band diagram of ITO/PEDOT/MEH-PPV/Au device, cathode being gold no electron will inject into the polymer under the influence of electric field.

As Gold work function is 5.1 eV which is near the HOMO level of the MEH-PPV (5.3 eV) it suppresses electron injection into the polymer, and it can be used as both anode and cathode for hole only devices. In the present study, ITO/PEDOT: PSS has been chosen as

anode because of it's highly transparency which is a requirement for anode in PLED. ITO also has a very good work function of 4.8 to 5.0 eV (ozone treated). To verify the nature of the hole current, the role of hole injection layer PEDOT has been studied.

3.2 Hole Only Diode Fabrication

All samples were prepared on square glass substrates (5 cm X 5 cm) covered with a patterned layer of indium-tin-oxide (ITO), which is transparent, so the light emitted by the LED can be collected. ITO has a work-function of 4.8 eV. This matches relatively well with the HOMO of the MEH-PPVs (5.2–5.3 eV) in order to form a nearly ohmic contact for the holes. Prior to spin coating of the organic layer(s) onto ITO, chemical and physical surface treatments were used to remove contaminants, smoothen the surface, and improve the ITO work function from 4.8 eV to 5 eV. The cleaning steps were as follows: rubbing with soap/detergent solution, rinsing with hot DI water, ultrasonic treatment in with DI water, spin-drying. Pattern the ITO substrates with proper enchants and define the pixel size with lithography or screen printing with epoxy in order to eliminate the edge effect (at edge there will be high electric field) finally UV-ozone treatment for 15 min. and hold for 10 min. ITO is a combination mixture of indium oxide and tin oxide, although it is widely used as an anode, has the disadvantage that oxygen diffuses into the organic active layer and contributes to the degradation of the device with time [5]. In order to improve the device stability and performance, a conductive and transparent layer of PEDOT-PSS consisting of poly (3, 4-ethylenedioxythiophene) (PEDOT) doped with polystyrenesulfonate (PSS) obtained from H.C.Starch Baytron P VPCH 8000 Germany, was filtered and spin-coated.

3.3   Role of PEDOT/PSS on Hole only devices

PEDOT/PSS Poly(3,4-ethylenedioxythiophene) doped with polystyrenesulfonate (PSS) is increasingly used in organic electronics because of its low band gap (1.65 eV) and a high work function of the order of 5.1 to 5.2 eV, which qualifies it as good electrode for

hole injection into a semiconductor with some interesting properties. PEDOT is aqueous dispersions of the intrinsically conductive polymer, it is based on a hetero cyclic thiophene ring bridged by a diether, this means it has the same conjugated backbone as polythiophene. It can be spin coated onto a huge variety of conducting and non conducting substrates including glass, ITO, silicon, chromium, gold etc., which gives a good formation of thin film.

Conductivity not only dependents on baking temperature but also on aqueous dispersions, the conductivity of the polymer conductor PEDOT: PSS doesn't change much in aqueous dispersions. For an electroluminescent (EL) polymer needs only a low intrinsic conductivity. This makes them easy to process into coatings, or for multilayer film applications in conjunction with organic semiconductors. Also, Film thickness changes due to decrease in viscosity at room temperature [6].

3.4 PEDOT coating on an ITO-Substrate

The use of PEDOT leads to a significantly improves overall device performance by smoothening of the anode surface and facilitating hole-injection. PEDOT is applied by common spin-coating techniques and is especially recommended for use in OLEDs and PLEDs due to reduced particle size and number of gel particles.

The ITO anode is cleaned thoroughly and ozone treated for 15 *minutes* and held for 10 *minutes* in ozone box. The thickness of the PEDOT layer coating onto ITO is determined by the following parameters:

- spin speed (max. of 1500 *rpm*)
- dilution of DI water
- Quality of the pre-conditioning of the substrate surface.

Before the PEDOT is deposited onto an ITO surface, filtering of the PEDOT solution is done using a fresh syringe equipped with new 0.25 μm filter in order to remove residual gel particles or dried particulates.

The PEDOT solution was spread to cover the entire substrate surface. During spin-coating, the substrate is held by a vacuum chunk (4 cm diameter). In general, the layer-thickness was found to be homogeneous across the substrate, with a somewhat increased thickness at the edges of the substrate. Different thicknesses of PEDOT/PSS ranging between 200-850 A^0 were coated to ascertain the role of PEDOT in hole only devices. After spin-coating, the PEDOT layer is dried for 90 $minutes$ at 120° C in vacuum chamber.

3.5   Barrier Contact with PEDOT: PSS

With the Ionization potential change the barrier height decreases due to the introduction of PEDOT: PSS. Where $\Delta\Phi_{p1}$ = 0.2-0.3 eV (Fig 3.1) $\Delta\Phi_{P1}$ is purely depended on the work function or Fermi level of the Metal ITO. Energy barrier $\Delta\Phi_{P1}$ not only depend on work function but also on plasma or ozone treatment [8]. And $\Delta\Phi_{p2}$ = 0.1 eV (from Fig 3.1). The overall $\Delta\Phi_P$ has decreased from 0.3 eV to 0.1 eV which specifies the high rate of hole injection in the emissive layer.
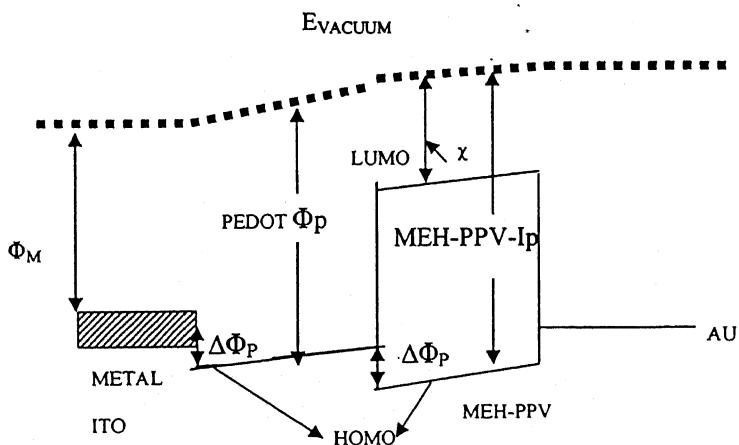
Fig 3.2: Energy band diagram for ITO/PEDOT/MEH-PPV/Au

$\Delta\Phi_{P1}$ is purely depended on the Fermi level of Metal ITO. On introduction of PEDOT

$\Delta \Phi_{P2}$ will be depend only on PEDOT HOMO level & independent of ITO E_F or E_c.

But for the organic conductor like PEDOT: PSS the Energy barrier $\Delta \Phi_{P2}$ depend only on $\Delta \Phi_{P1}$.

The active organic layer was spin coated from MEH-PPV (Al'drich) filtered solution with a spin speed rates of 800 rpm in a nitrogen atmosphere. The polymer thickness varied around 800 A^0 measured by Alpha step 500 profiler. The coated sample was placed in a centrifugal spin dry for 7 min and vacuum baked for $120^0 C$ for 2 $hours$. The solvent used for MEH-PPV were 6 mg/ml solution of xylene and chloroform. The polymer solution was well stirred on magnetic stirrer for 24 $hours$ and optionally heated at 45^0–$60^0 C$.

The layer thickness was measured using a Tencor Alpha-step 500 surface profilometer. The gold metal for cathode was thermally evaporated on the sample inside a vacuum system at typically $10^{-6}\,mbar$, typical thickness 2500 A^0. Diodes with different PEDOT thickness of 0 A^0, 200 A^0, 500 A^0, 700 A^0, & 850 A^0 respectively were fabricated for understanding the role of PEDOT thickness on the performance of the device.
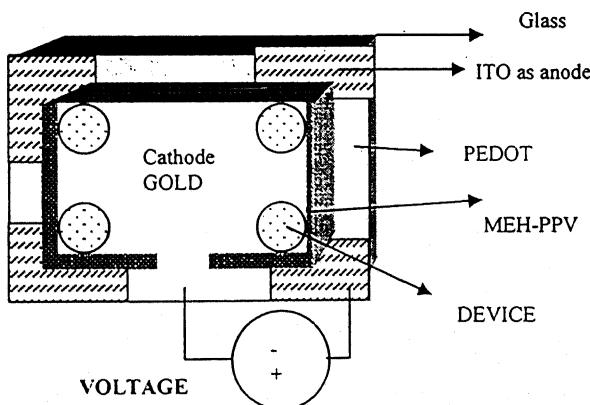
Fig 3.3: Hole only diodes with gold as cathode

The samples were encapsulated with getter. The resulting sample consisted of four independent devices of same area of 0.5 cm^2.

3.6 Results & Discussion:

In these experiments of hole only devices with different PEDOT thickness, the main observation is the effect of PEDOT thickness on the yield of the devices. Our observations are summarized in table 3.1 and 3.2.

3.6 (a) Role of PEDOT on hole only devices (YIELD)

With PEDOT a conducting polymer, the yield details are given below with different thicknesses:

<table>
<tr><td colspan="5">Table 3.1 Effect of PEDOT thickness on the yield of the devices</td></tr>
<tr><td>PEDOT
Thickness</td><td>No. of devices
Fabricated</td><td>No. of devices
good</td><td>No. of devices
short</td><td>No. of devices
uncertain</td></tr>
<tr><td>850 A^0
(undiluted)</td><td>28</td><td>22</td><td>2</td><td>4</td></tr>
<tr><td>700 A^0</td><td>16</td><td>8</td><td>5</td><td>3</td></tr>
<tr><td>500 A^0</td><td>12</td><td>5</td><td>6</td><td>1</td></tr>
<tr><td>200 A^0</td><td>20</td><td>7</td><td>10</td><td>3</td></tr>
</table>

3.6(b) Advantages of using PEDOT layer in PLED:

An intermediate layer of PEDOT: PSS improves the yield, and smoothing of surface near the active polymer.

[1] Smoothening of anode surface& facilitating hole injection.

[2] Electric shorts in PLED devices can be reduced.

[3] The forward current below turn on voltage in the PEDOT/MEH-PPV devices is comparatively lower than the MEH-PPV only devices of the I.D.Parker [4].

3.6(C): Surface roughness: Surface roughness measured on Alfa step 500 surface profiler.

Table 3.2: Effect of PEDOT on surface roughness	
PEDOT thickness	**Roughness**
850 A^0(pure)	Up to 20 A^0
500 A^0	Up to 40 A^0
0 A^0	Up to 120 A^0 (ITO)

From the table 2.1 and table 2.2 suggest that with the thicker PEDOT the yield of the devices is high, because the surface roughness is changed from ITO to PEDOT and the roughness of PEDOT is less compared to the surface roughness of ITO. Also the increase of PEDOT thickness the surface roughness of PEDOT will decrease. Hence it is worth while to use thicker PEDOT for the PLEDs/OLEDs.

3.6(d): Characterization of Hole only devices

The experimental J-E characteristics of hole only device as a function of PEDOT: PSS layer different thicknesses, the current densities in Log-Linear scale are shown below in Fig- 2.10. The devices characteristics measured by Labview 7.1.
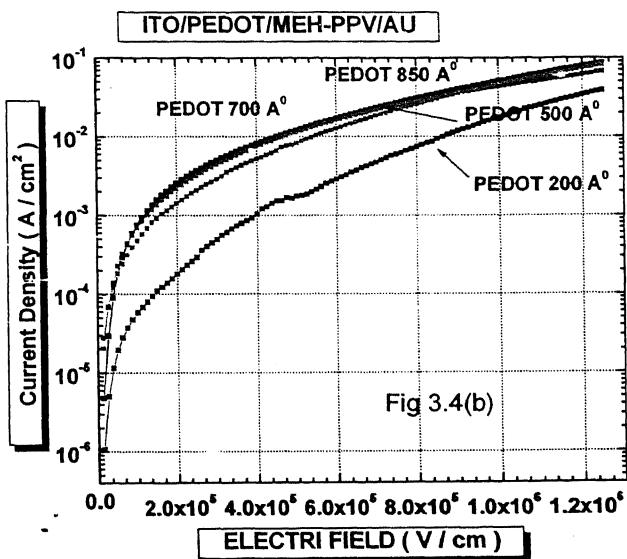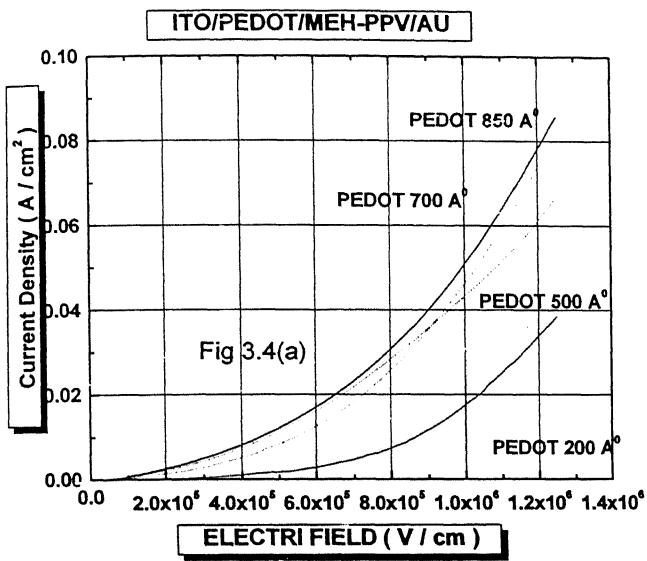
Fig 3.4: Experimental _J-E_ characteristics of ITO/PEDOT/MEH-PPV/Au hole only device in (a) linear-linear (b) log -linear scale, measured by Labview 7.1.

The experimental results of these devices show a small dependence of variations in the range between 500 to 850 A^0. The current density of 200 A^0 is small compared to the other devices of the hole only diodes. The magnitudes of the current densities of these devices show almost same.

The data shown in the top diagram on a Log – Linear scale are plotted on a Log – Log scale in the bottom diagram for better differentiation. This scale can predict the presence of space charge limited current. The experimental _J-E_ characteristics of ITO/PEDOT/MEH-PPV/Au, hole only device are shown below in Fig 3.5
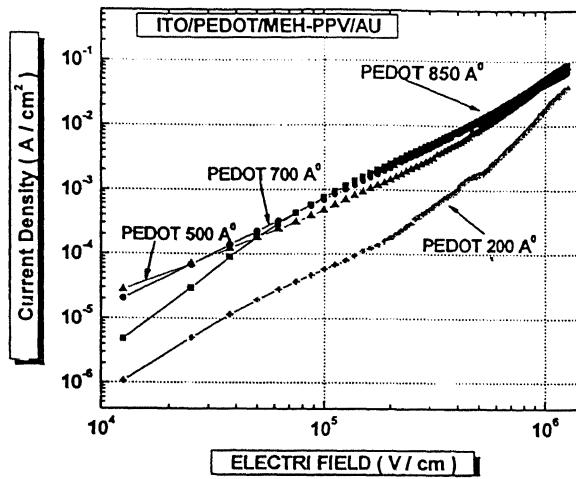
Fig 3.5: Experimental *J-E* characteristics of ITO/PEDOT/MEH-PPV/Au hole only device with different PEDOT thickness, in log-log scale.

The results of the Fig 3.5, shows the linear dependence in log-log scale, which is space charge limited. The slopes of these curves are shown below in table 3.3.

Table 3.3: The slope of the different PEDOT thickness based on Fig 3.5.

Slope at Electric field(Horizontal) → PEDOT thickness ↓	Slope In the range of $10^4 - 10^5$ *(V/cm)*	Slope In the range of $10^5 - 10^6$ *(V/cm)*	Slope In the range of $10^4 - 10^6$ *(V/cm)*
850 A^0 (undiluted)	1.87	2.44	1.93
700 A^0	1.7	1.84	1.78
500 A^0	1.36	2.12	1.90
200 A^0	1.90	2.76	2.4

The slopes of the different PEDOT thicknesses shown for the low fields i.e of the similar dependence of the current at low fields at 10^5 *V/cm* the current is not consistent due to thermionic emission, from the electric field, 10^5 to 10^6 *V/cm* the current is space charge region and greater than 10^6 *V/cm*, the current is not space charge limited and the current is increasing more.

To know clearly fields greater than 10^6 *V/cm*, FN-tunneling is plotted in Fig 3.6
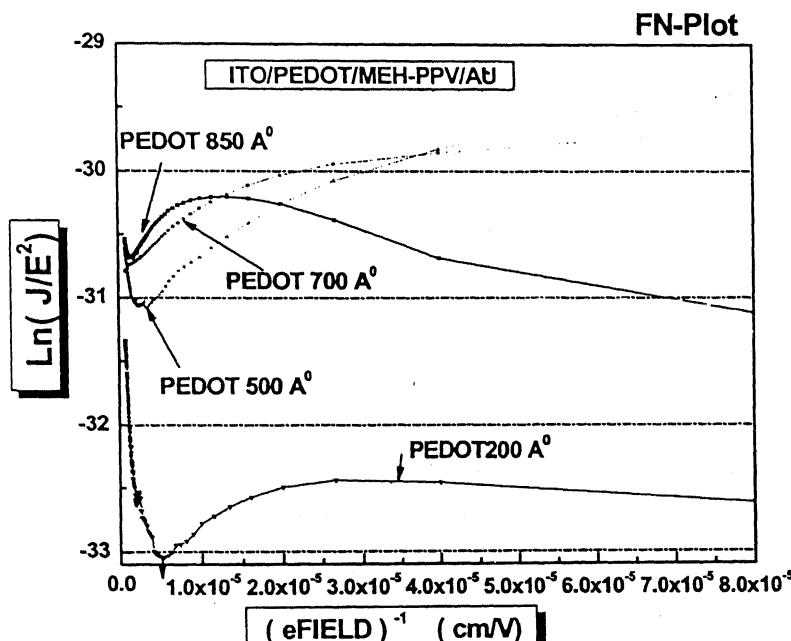
Fig 3.6: Fowler–Nordheim plot for ITO/PEDOT/MEH-PPV/Au, hole only device, the slop shows injection barrier height at high electric field

In Fig 3.6, FN-plot shows a negative slope at higher electric fields, suggesting the field emission phenomenon occurrence in all the devices of different PEDOT thicknesses.

This field emission leads to barrier lowering, in Fig 3.6 shows the closer look of Fig 3.7, to find the slope and the barrier height.
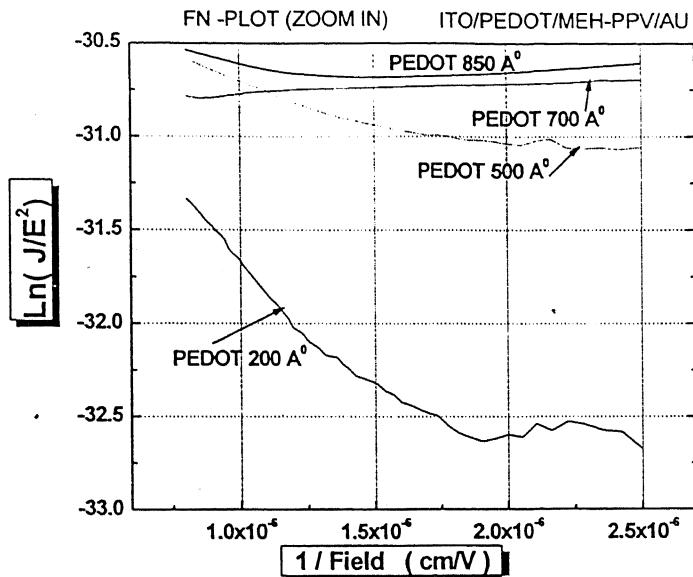
Fig 3.7: Fowler-Nordheim plot for an 800A⁰ thick MEH-PPV, hole only device at higher electric fields. (Zoom in of above Fig.)

The shape of $Ln(J/E^2)$ vs $1/E$ curves from the data given in Fig 3.7, suggests a barrier for hole transport at the interface. The slopes of different PEDOT thicknesses show different slopes, and contact barrier heights are measured by high field FN-tunneling and are plotted in the table 3.4. In the above analysis we have ignored any effect of image force on the barrier shape.

Table 3.4: The variation of PEDOT thickness, calculation of barrier height with slopes at fields greater than 2e6 with FN—tunneling equation no.(6); considering the work functions of ITO, PEDOT and HOMO of MEH-PPV is 4.9 eV, 5.1 eV and 5.2 eV respectively

PEDOT Thickness	Slope	Barrier height Measured (Φ_e eV)
$200 \ A^0$	-1.17e6	0.147
$500 \ A^0$	-5.3e5	0.067
$700 \ A^0$	-4.5e5	0.060
$850 \ A^0$ (undiluted)	-3.1e5	0.052

We find that for different PEDOT thicknesses (200 A^0 to 850 A^0) Φ_e is varying from 0.147 to 0.052, as shown in table 2.4. For the thicker PEDOT i.e. in the range of 500 A^0 to 850 A^0 the contact barrier height is small compare to the thinner PEDOT of 200 A^0. All these measurements were taken at greater fields i.e. 10^6 V/cm.

Thus we estimate that the SCLC observed in all our hole only devices arises from the fact that the injection barrier at the PEDOT—MEH-PPV interface is less than 0.15 eV. The results of Parker [4] for hole only device was given by FN-tunneling (field emission) because of the barrier height was around 0.5 eV high, since their device was ITO/MEH-PPV/Al (i.e. not used PEDOT:PSS). The results depicted in this study given by Fig.3.11, the slope of the Log (J)–Log (E) plot :we observe that the current density depends quadratically on the field. This behaviour is characteristic for space charge limited current in which case given by equation no.2.

3.7 Summary:

Hole only diode, the nature of current can be classified into three regions: - linear region where the electric field is less than 10^5 *V/cm*, space charge region from 10^5-10^6 (*V/cm*), and field emission region greater than $2x10^6$ (*V/cm*). For high yield, PEDOT thickness should be high enough so that it reduces the roughness from ITO (roughness of 120 A^o) to PEDOT (roughness of 20A^o). With the introduction of PEDOT the roughness is dependent on PEDOT only not on ITO. By measuring the hole current in hole only devices we can know the magnitude of hole current flowing in a ITO/PEDOT/MEH-PPV/Ca/Al device. We have also shown, that an intermediate layer of PEDOT: PSS enhances yield of the polymer devices. The yield increases with increase in the thickness of the PEDOT layer.

CHAPTER IV

Study of Electron Only Device (Mg/MEH-PPV/Ca/Al)

4.1 Introduction

In order to know the nature and magnitude of electron current in a PLED, one has to fabricate the electron only device, and measure the current. Replacing the ITO & PEDOT contact in an ITO/PEDOT/MEH-PPV/Ca/Al with Mg low work function metal gives devices in which the carriers are almost exclusively electrons, due to the large offset between the work function of the anode and the HOMO level of MEH-PPV [4, 13, 14].

Understanding the electron only current in a PLED is difficult because of the use of the low work function metals like Mg, Ca, Nd, etc., replacing ITO as anode, these metals gets oxidized in ambient environment within a few minutes. The fabrication of these devices is relatively more involved as compare to hole only devices.

4.2 Electron Only Diode

In an electron only device the carriers are electrons only and holes are insignificant. In order to investigate the electron current in a MEH-PPV device, the hole current needs to be suppressed. The low work function of Ca, Mg, or Nd electrode is expected to form a large barrier for injection of holes into MEH-PPV. In our experiments considering the convenience of evaporation and availability we have chosen Mg as the anode material. In the Fig.4.1, an energy band diagram of such a device is shown. In forward bias, the nature of electron injection into MEH-PPV from the Ca/Al electrode is studied.
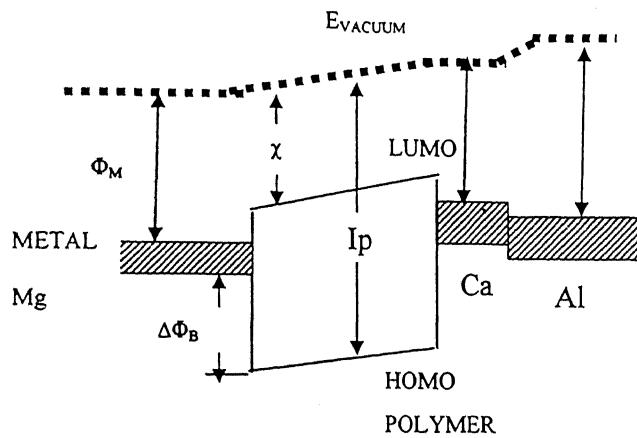
Fig 4.1: Energy band diagram for Mg/ MEH-PPV/Ca/Al

In forward bias, the electrons will be injected into the active layer of the device, while hole not injected due to large offset ($\Delta\Phi_B \approx 1.64$ eV) between the work function of the anode(3.66 eV) and the HOMO of MEH-PPV (5.3 eV). The current in this device is almost exclusively determined by the electrons injected at the Ca contact, the hole injecting contact plays no part in determining the I-V characteristics of these devices.

4.3   Electron Only Diode Fabrication

All samples were prepared on a soda lime glass consist of small fraction of sodium ions which are highly mobile, try to penetrate into the next layer, therefore the glass is covered with a small layer of SiO_2 to overcome the penetration. On the top of SiO_2 layer ITO is coated, the ITO metal is stripped off in an etching solution of $225:60:15$ ml of DI water, HCL, and HNO_3 (Nitric acid) at a temperature of $60\text{-}70^0 C$ for 10 *minutes* bath. Rinsing the substrates in DI water and cleaned in RCA solution to remove contaminants. The cleaning steps were as follows: rinsing with hot DI water, ultrasonic treatment in with DI

water and spin-drying. The samples were heated in a vacuum chamber for 30 *min* at 120^0 C and the Mg was thermally evaporated on to the glass plates with the metal masks. It was thermally evaporated by sublimation and the thickness of the Mg was 5600-8400 A^0. Mg was not very uniform on the substrate and some times some pin holes were also visible.

4.3.1   Difficulties of coating Mg on glass

[1] The rate of deposition was not under control because it sublimes too rapidly.

[2] It deposited on all the heated part and did not deposit on cold parts, such as glass bell jar

[3] Surface roughness was too high (nearly $1000A^0$)

[4] The deposition was not uniform on the substrate

After the deposition of Mg, epoxy was screen printed (as discussed in chapter 3). MEH-PPV (Al'drich) solution is prepared with 6 *mg/ml* solution of xylene and chloroform. The polymer solution was well stirred on magnetic stirrer for 24 *hours* and optionally heated at $45–60°C$. The MEH-PPV is coated on the Mg anode, with a spin speed rates of 600 *rpm*, and with a filter under low light in order to prevent photooxidation of the organic layer due to presence of light and oxygen. The polymer thickness was typically 800 A^0 measured by profilometer. The polymer coated sample was vacuum baked for $120^0 C$ for 2 *hours* for solvent removal.

The metals like Calcium, magnesium, aluminum are used as cathode in organic LEDs because of its low work functions in the order of 2.87 to 4.1 *eV*, which qualifies them as good electrodes for electron injection into polymer. Ca is a good conductor which is highly used as cathode with Al coated on top on it. Ca has Fermi level (or work function) is close to LUMO of active polymer. The top-cathode was thermally evaporated at a slow rate on the sample inside a vacuum system at typically 10^{-6} *mbar*, because at high rate of evaporation the temperature of the filament in which Al was loaded will be high, so that the atoms form the filament will be having higher kinetic energy. These atoms with high

kinetic energy can damage the polymer; hence we keep at low evaporation rate. Ca/Al metal is used as cathode for electron-only diodes with different Ca thickness of 0 A^0, 20 A^0, 50-85 A^0, & 200 A^0 respectively. The getters which are used for the encapsulation of the device are packed in a foil and heated for 2 *hours* at 180^0-200^0C in nitrogen flow for first 30 *minutes* and forming gas (85% nitrogen + 15% hydrogen) flow for the remaining time. These getters are the copper oxide a catalyst on activated can absorb oxygen and molecular seeds on activated can absorb moisture. These encapsulated devices are followed by the UV treatment for 20 *minutes*. The resulting sample consisted of four independent devices of same area of 0.5 cm^2. Thickness measurement of cathode was done by crystal thickness monitor, during evaporation.
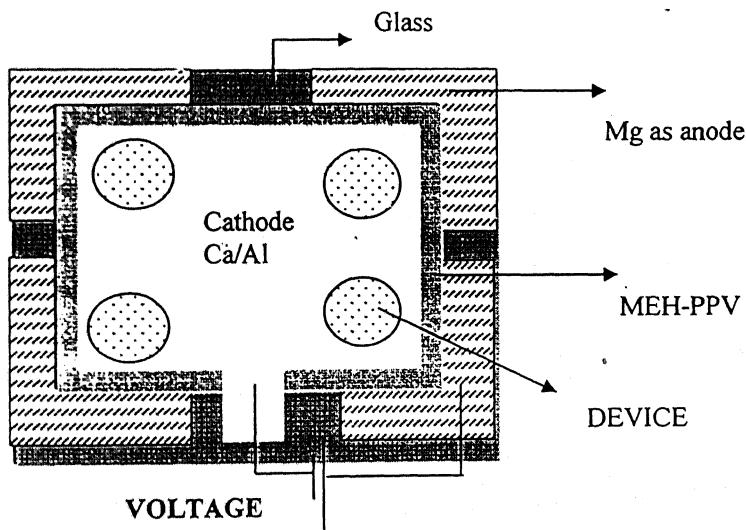
Fig 4.2: Electron only diodes with magnesium as anode and Ca/Al as anode.

4.4   Results & Discussion:

4.4(a)   Yield of Mg on Electron only devices (Mg/MEH-PPV/Ca/Al)

In this experiment, as the Mg deposition was difficult, yield of these devices was poor, so the large no of devices were fabricated for the study. The following table 4.1 shows the yield of the devices.

Table 4.1: With Mg as anode, the yields of the devices details are given below for different thicknesses of Ca:

Ca thickness	No. of devices fabricated	No. of devices good	No. of devices short
$200\ A^0$	32	11	21
$50\text{-}85\ A^0$	28	8	20
$20\ A^0$	20	9	11
$0\ A^0$	16	10	6

4.4(b):   Nature of Electron current in Electron only device

For the fabricated devices, the *I-V* characteristics have been measured using LabView [Appendix-A].The data acquired by Lab-View, are plotted in Origin have been shown below.
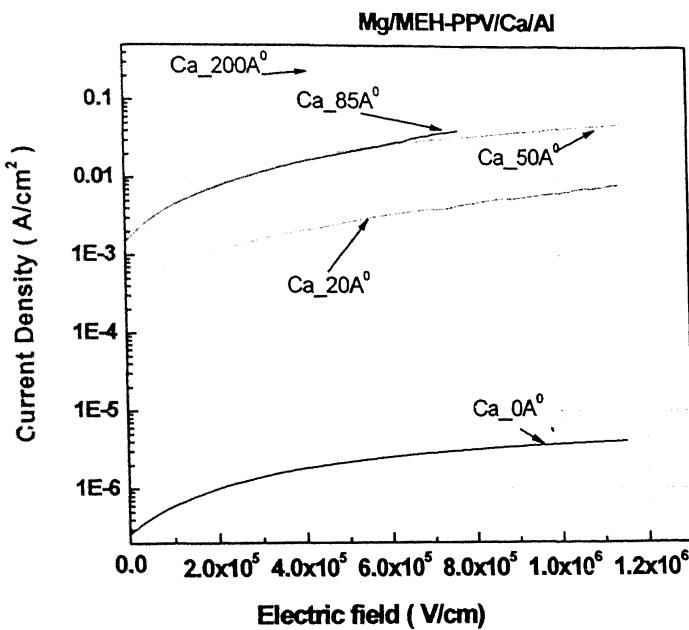
Fig 4.3: Characteristics of Mg/MEH-PPV/Ca/Al Current Density *(A/cm²)* verses Electric field *(V/cm)* in log –linear scale

The current density of cathode Al (Ca=$0A^0$) is 3 order of magnitude less in comparison to the smaller thickness of Ca - $20A^0$ cathode as shown in Fig 4.3. With in the Ca thickness range of 20-$200A^0$ there is a 2 order of magnitude difference. As the Ca thickness increases the current increases significantly, the nature of electron current is difficult to understand and analyze in Log-linear scale.

To determine the space charge limited current, the current density is proportional to the square of the electric field (voltage) in SCLC (*i.e. J α E²*). In log-log scale this becomes a straight line with slope 2. So can be easily determined whether the current density is space charge limited or not.

For better understanding the same graph in Fig 4.3 is plotted in Log-Log scale in Fig 4.4.
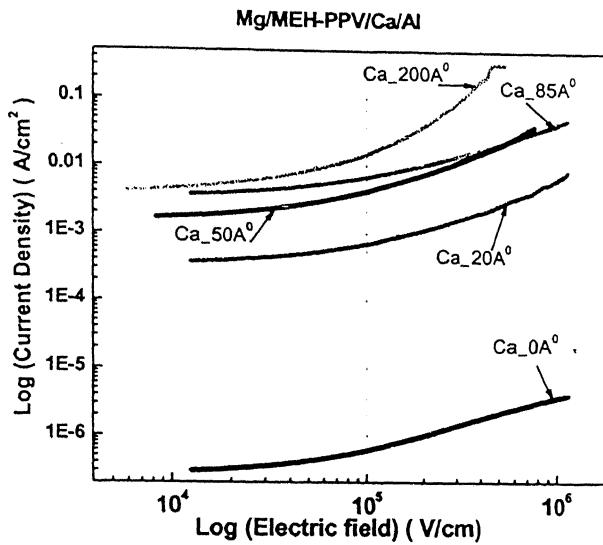
Mg/MEH-PPV/Ca/Al

Fig 4.4: Experimental Characteristics of Mg/MEH-PPV/Ca/Al) in log-log scale.

Looking at graph Fig 3.4, the slope in the entire region is not constant, so we have tried to determine in different region. This information is summarized in table 4.2.

Table 4.2: From the Fig 3.4 the slopes of the different devices are given below as a function of electric fields.

Ca thickness in A^0	10^4-10^5 (V/cm)	10^5-10^6 (V/cm)	10^4-10^6 (V/cm)
0	0.34	0.82	0.72
20	0.3	1.06	0.85
50	0.38	1.14	0.87
200	0.55	1.99	1.19

The nature of current density of different Ca thickness show different signature in different electric field region as shown in Fig 4.4. From table 4.2 the Ca thickness below 200 A^0 the current is not space charge limited. While for Ca thickness 200 A^0 in the field region of 10^5-10^6 (V/cm), the current is space charge limited, the slope is around 2. For the electron only devices at less than 10^4 (V/cm) the current is not space charge.

The device of our interest is Ca 200 A^0 because of its space charge behavior. The slope of this device is linear fitted with fitting parameters as shown below.
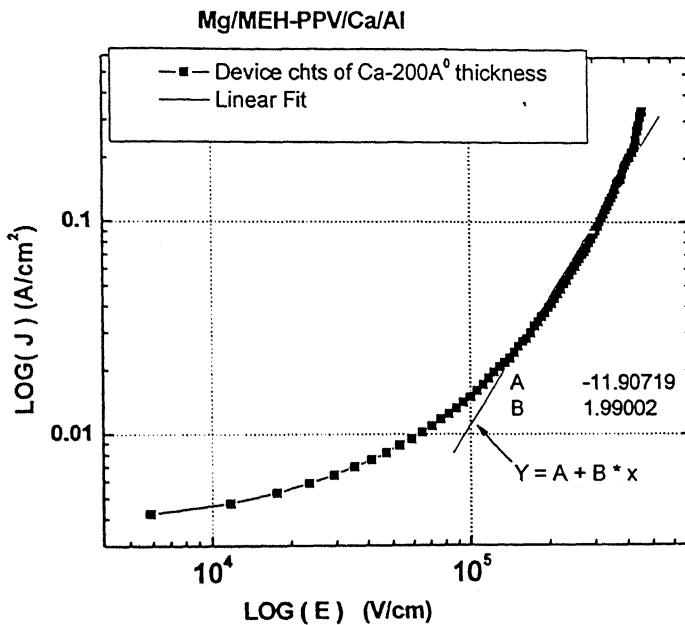
Mg/MEH-PPV/Ca/Al

Fig 4.5: Characteristics of Mg/MEH-PPV/Ca/Al Current Density (A/cm^2) verses Electric field (V/cm) in log-log scale of Ca 200 A^0 with a slop of 1.99.

From Fig 4.5, *J-E* characteristics resulting from injection at Ca contacts are well fitted by theory for space charge limited with reasonable values for the variation of fields. It is clear, that beyond a certain electric field the current density is even high than what is predicted by SCLC. The addition current density can be due to field emission (FN-tunneling) which is activated when the field crosses some threshold value. One has to draw FN plot to ascertain whether there is FN tunneling mechanism active or not.
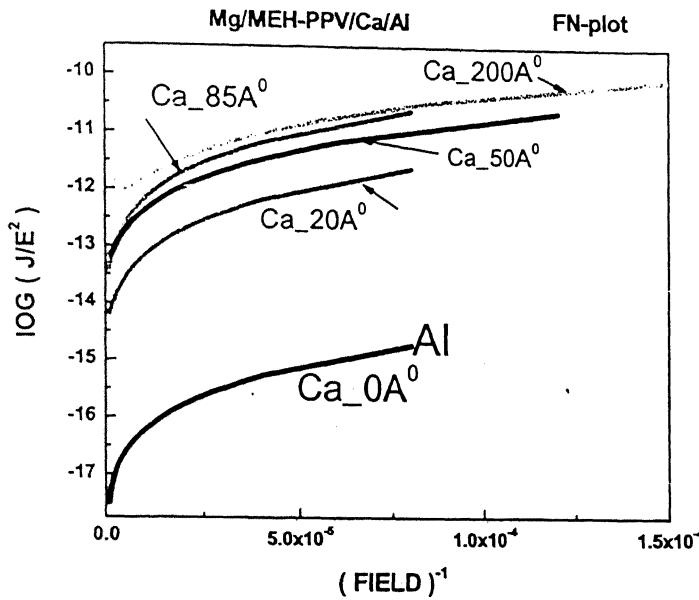
Fig 4.6: FN-tunneling Characteristics of Mg/MEH-PPV/Ca/Al of different Ca thickness

From Fig 4.6, shows the FN-Plot for all the electron only devices. Here it is clear that for less than 200 A^0 thicknesses no FN tunneling is observed in electron only devices. For Ca thickness $\approx$ 200 A^0 we observe that at electric field greater than 4 x 10^5 V/cm, there is a small knee is observed and current is showing the nature of FN tunneling. In Fig 4.7 to better understanding this region of electric field greater than 4 x 10^5 V/cm, it has been expanded.
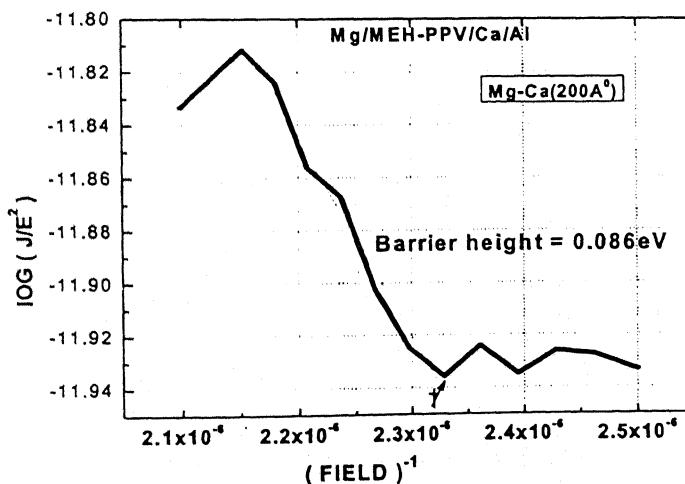
Fig 4.7: FN-tunneling for above device (i.e. 200A^0 Ca thick) shows barrier height of 0.086 eV,
† the knee in the curve is around 3.5 V.

Using the method outlined previously (i.e. in chapter 3), the barrier height is calculated which comes out to be 86 meV. But the theoretical barrier height is 130 meV, as the work function of Ca is 2.87 eV and LUMO level of MEH-PPV is 3 eV.

4.4(c):   Characterization of Hole only and electron only devices

The hole current obtained by hole only device of PEDOT thickness of 850 A^0 and electron current obtained by electron only device of Ca thickness of 200 A^0 has shown space charge limited current in the filed region of 10^4 to 10^5 V/cm and 10^5 to 4 x 10^5 V/cm respectively as shown in Fig 3.8(a).
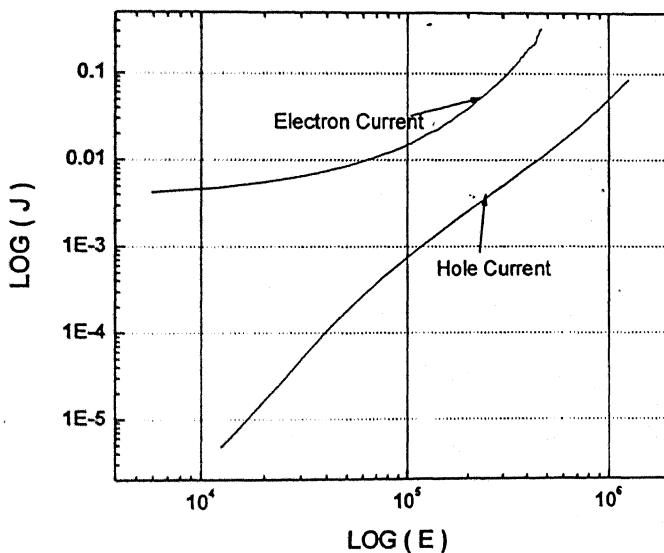
Fig 4.8(a): *J-E* Characteristics of both devices i.e. hole only device and electron only device

The total current in a composite device can be a combination of the electron current and hole current as shown in Fig 4.8 (b).
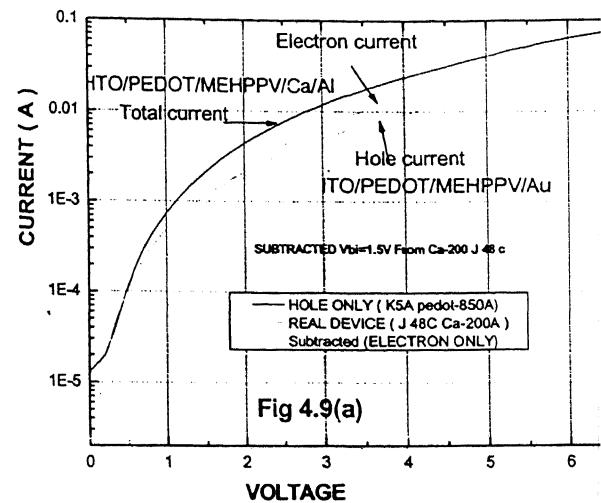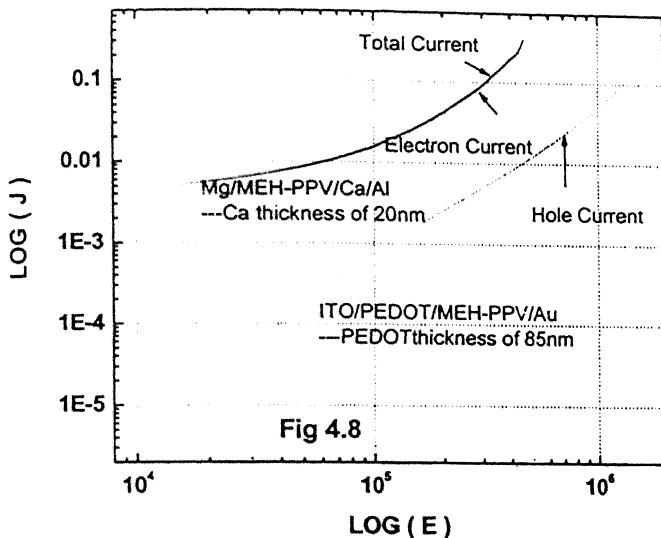
Fig 4.8(b): *J-E* Characteristics of both devices i.e. hole only device and electron only device and the interpolated total current.

Fig 4.9(a): Finding the electron only current, by subtracting the hole current from the PLED. The hole device and the Real device have the same thickness of 800 A^0 and the device area is also same of 0.5 cm^2

Another way of knowing the electron current, is to fabricate the ITO/PEDOT/MEH-PPV/Ca/Al, PLED and find the total current and subtract the hole current from it as shown in Fig 4.9. But the fabricated total current is not equal to the sum of both the currents.
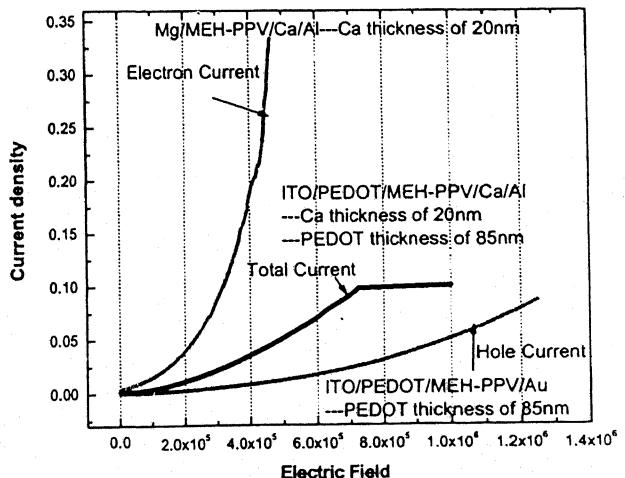
Fig 4.9 (b): All the three currents shows that the total current is not the sum of electron and hole current.

43

This method of subtracting the hole current from the total current in a PLED may not be acceptable. In a real device one kind of current may be influenced by the presence of charge carriers of the other kind by the charge modulation of the electron current and hole current respectively.

4.4 (d): Results of PLED (ITO/PEDOT/MEH-PPV/Ca/Al) device

In electron only device and hole only device only one class of carriers had been flowing in the device. For a light output device it is necessary to inject both the carriers from different electrodes. The nature of hole currents of different thickness and Calcium thickness of 200 A^0 are space charge limited, but for the bipolar carriers in a PLED the current is not the space charge limited in these fields.

These devices are fabricated with the PEDOT layer of 850 A^0 and different Ca thickness. The characteristics of these devices are shown below in Fig 4.10.
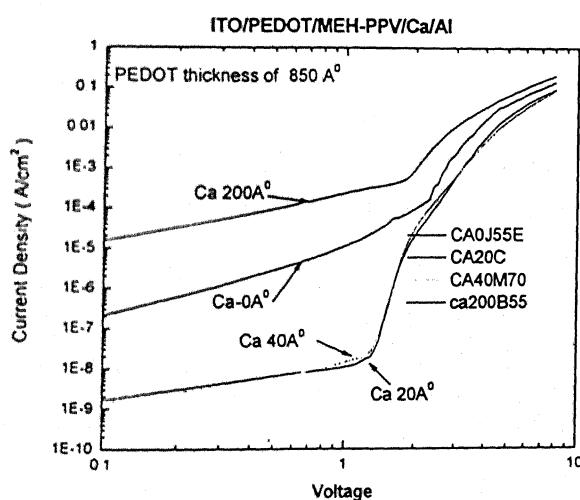
Fig 4.10: Experimental J-E characteristics of different Ca thickness of PLED (ITO/PEDOT/MEH-PPV/Ca/Al).

These devices are giving light output from 1.8 V onwards. Without Ca the light output was greater than 4 volts. The nature of current of these devices is not space charge limited. To further investigate FN-tunneling for these devices, Fig 4.11 is plotted. The field emissions of different thickness are activated at different fields as shown in table 4.3.
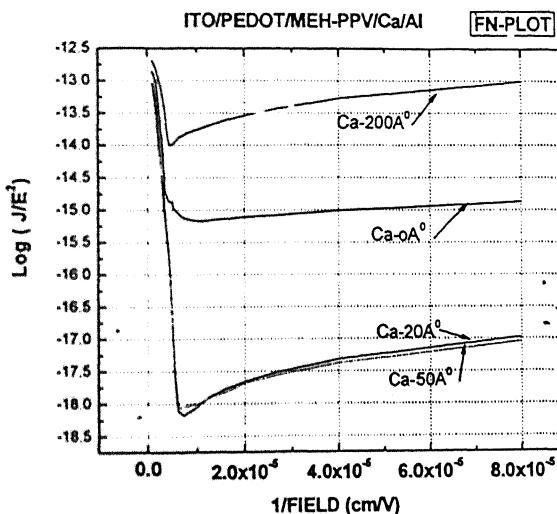
Fig 4.11: FN-tunneling for all device of PEDOT 850 A^0 & different thickness of Ca thickness.

The calculated field of these devices are shown in the Table 4.3

Table 4.3: Field emission for different calcium thickness and PEDOT of 850 A^0 as shown in Fig 4.11, calculated its start at fields given below.

Calcium thickness in A^0	Field emission activated at field (V/cm)	Voltage (V) at the start of field emission
0 (i.e. Aluminum)	5.8×10^4	0.464
20	7.6×10^4	0.608
50	7.7×10^4	0.616
200	1.06×10^5	0.848

From this table 4.3, it is clear that in a PLED (ITO/PEDOT/MEH-PPV/Ca/Al) of different thickness of Ca the FN-tunneling is occurring at very low fields (voltages) and as the thickness of the Ca increasing the initiate of field emission is also increasing its filed.
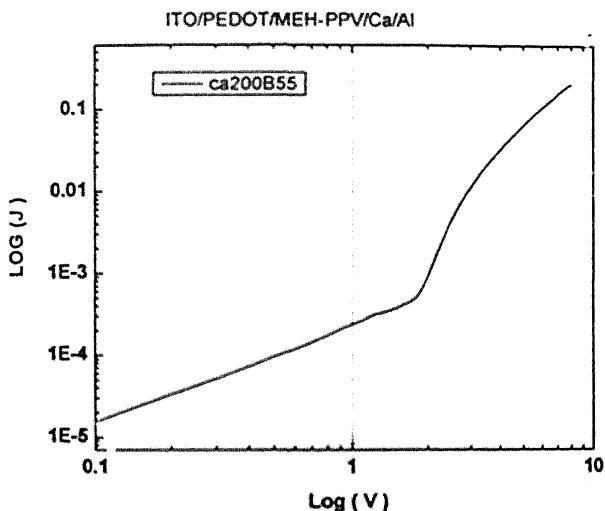
Fig 4.12 (a)
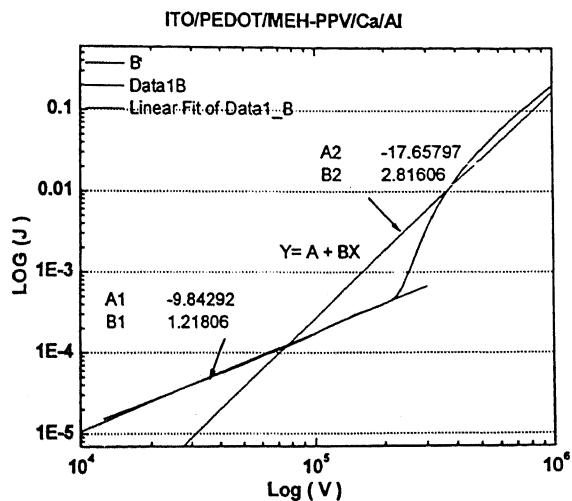
Fig 4.12 (b)

Fig 4.12(a): Experimental *J-E* characteristics of PEDOT 850 A^0 and Ca 200 A^0 thickness of (ITO/PEDOT/MEH-PPV/Ca/Al). (b) Linear fit for the 2.2 x 10^5 (*V/cm*) (i.e. 1.8 *V*) and above this field the current is polynomial fit.

In this device, at low electric fields the current densities are linear. At high voltages the current is not space charge limited. FN-tunneling for all these devices shown in Fig 4.11, the device of our interest is PEDOT thickness of 850 A^0 & Ca 200A^0 the graphs of different plots are given in Fig 4.12.

The FN-tunneling for the ITO/PEDOT/MEH-PPV/Ca/Al with Ca thickness of 200 A^0 are given in Fig 4.13 the barrier height for this device is difficult to predict; it may be due to electrons or holes.

46
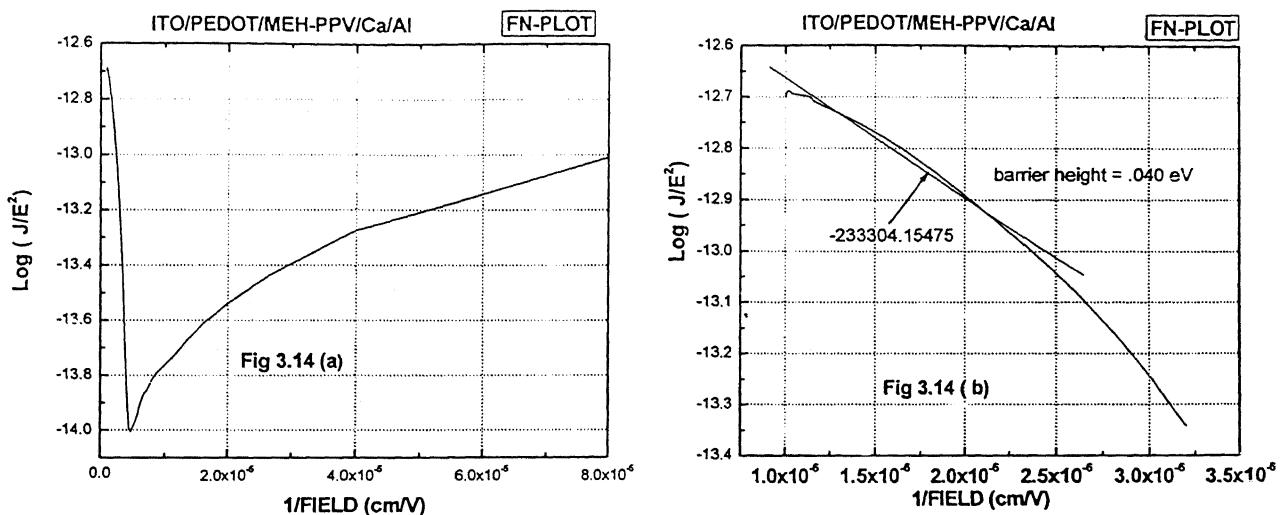
Fig 4.13: FN-tunneling for above device (i.e PEDOT 850 A^0 & 200 A^0 Ca thick) shows barrier height of 0.04 eV, the start of field emission the curve is around 2.5 V.

The nature of electron current density for these PLEDs of different thickness of Ca, are not the space charge limited current because from the results the slopes of log-log curve is not equal 2, and at lower fields the current is due to leakage current .

4.5   Summary:

The nature of electron current in electron only devices are not the space charge limited nor the field emission for the Ca cathode thickness of less than 200 A^0. For only Ca thickness of greater than or equal to 200 A^0 of thickness the current is space charge limited in the field region of 10^5 to 4 x 10^5 V/cm. Beyond that the current is dominated by field emission. For a PLED of ITO/PEDOT/MEH-PPV/Ca/Al device the currents are dominated by the FN-tunneling, at low fields the currents are due to leakage or thermionic effects.

LIFT-OFF PROCESS WITH POSITIVE PHOTO RESIST

5.1   Introduction to the Lift-Off process

Photolithography is the optical process of transferring geometric shapes from a mask to the surface of a substrate. Positive resist undergoes bond breaking when exposed to light, while negative resist form bonds or cross-links between polymer chains under the exposure. To patterning the metallization of cathode for isolation between two metal lines there are three processes:- Metal mask, Metal etch(wet/dry) and Lift-Off . Metal or shadow mask works best for the large area of metal deposition since the creation of mask will be easier for mask designers. But as the size of the mask decreases it is difficult to design metal mask, hence resolution decreases. Metal etch is of two types - wet etch and dry etch, and comprises four basic processes. Initially the metal is evaporated all over the substrate followed by the patterning using photoresist film. After lithography the metal is etched by an acid with the removal of photoresist. In its place, a rather sophisticated lift-off technique was developed, prior to metal deposition, photoresist is applied to the substrate and baked. The photoresist is patterned in such a way that it ends up beign negative sidewall after development. This then "shadows" the deposition of the metal films, resulting in much superior lift-off.

Lift-Off process needs no etching; it inherently offers cost, density and negative sidewall advantages. In this thesis "Image Reversal Process" has been studied.
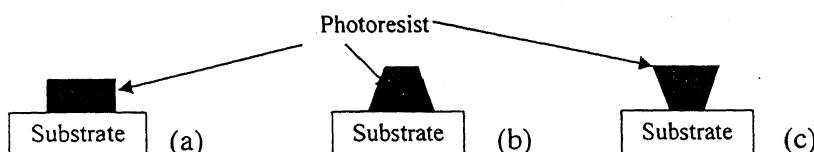
Fig 5.1: Photoresist after the lithography process

(a) Normal Process (b) Positive sidewall (c) Negative sidewall

5.2   Potential of Lift-Off process in OLED/PLED cathode lines

Organic light emitting diodes are the heart of the passive matrix display, with an emissive polymer sandwiched directly between high and low work function metals. In PLEDs/OLEDs anodes are chosen as transparent materials and the top layers cathode are opaque. In a matrix display there are many pixels of OLED/PLED and cathode lines must be isolated with neighboring electrodes in order to reduce the shorts and cross talk such that each pixel will be independent on its sources.
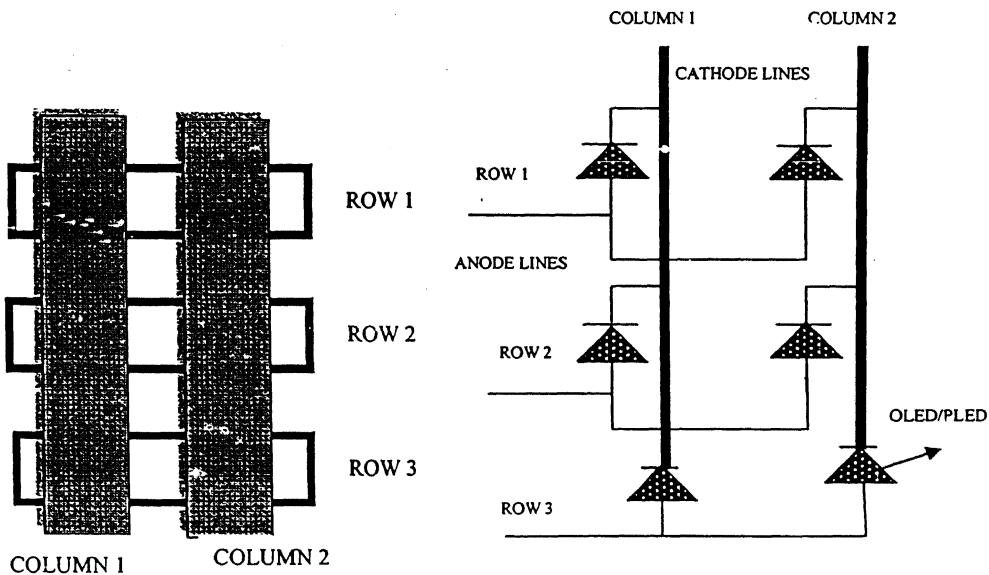
Fig 5.2: Passive matrix display with rows as anode lines and column are as cathode lines

The separation of cathode lines in passive matrix displays can be done by Lift-Off - image reversal process, where the photoresist requires a negative slop (negative sidewall) in order to conform, to the metal isolation, and in OLED/PLEDs photoresist is not necessarily lifted off after the deposition of metal.

5.3   Lift-Off Process: Chlorobenzene soak

Lift-Off process in chlorobenzene soak is anisotropic etch process [22]. In this process it is difficult to control soak time and reproducibility is difficult to achieve. Use of toluene and chlorobenzene are hazardous. In the Fig 5.3: lift-Off using chlorobenzene soak process is given.
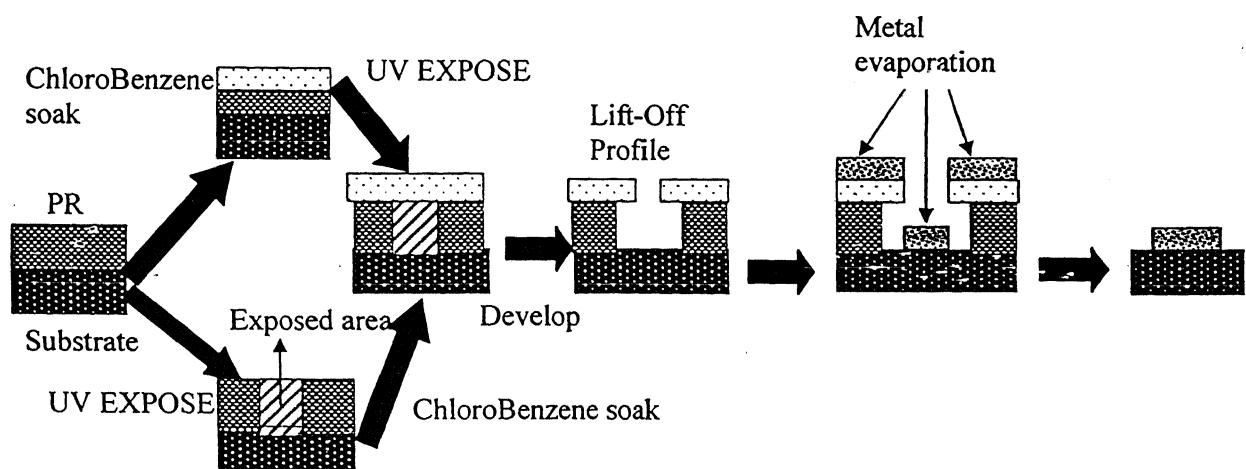
Fig 5.3: Lift-Off processes in Chlorobenzene soak

5.4   Lift-Off process By Image reversal

Image reversal is a chemical process by which a positive photoresist is made to behave like a negative photoresist. Positive photoresist (PPR) has the advantages of high contrast, good step coverage, and high aspect ratios. PPR is a radiation sensitive material consisting of three constituents, viz. 22% alkaline soluble base resin, 8% a photosensitive dissolution inhibitor (often called the Photosensitive or Photo-Active Compound (PAC)) and 70% of a carrier organic solvent. The photoactive compound in its initial state is an inhibitor of dissolution. Once this photoactive dissolution inhibitor is destroyed by light, the resin becomes soluble in the developer.

The working mechanism of positive photoresist is as follows - The PAC is a diazoketone which upon exposure to ultraviolet (UV) radiation generates a highly reactive intermediate ketone and liberates nitrogen. The ketone will react with available water to form an indene carboxylic acid which is now soluble and can be developed. In the above process the novolac-type resin is basically unchanged, and its solubility is controlled by the presence of either the dissolution inhibitor or enhancer. The degradation of dissolution enhancer can be utilized for the reversal of the resist image. 3

In a reversal process imidazole is added to the positive photoresist. Upon UV exposure Imidazole, the novalak resin and PAC will change to the novalak resin and soluble acid (i.e. PAC changes to soluble acid). When baked the soluble acid changes to insoluble derivative. Now under the flood exposure (without the mask) the remaining PAC which was covered by mask previously will transform to a soluble acid. After development this creates a negative pattern on the substrate [20,21,23,24].
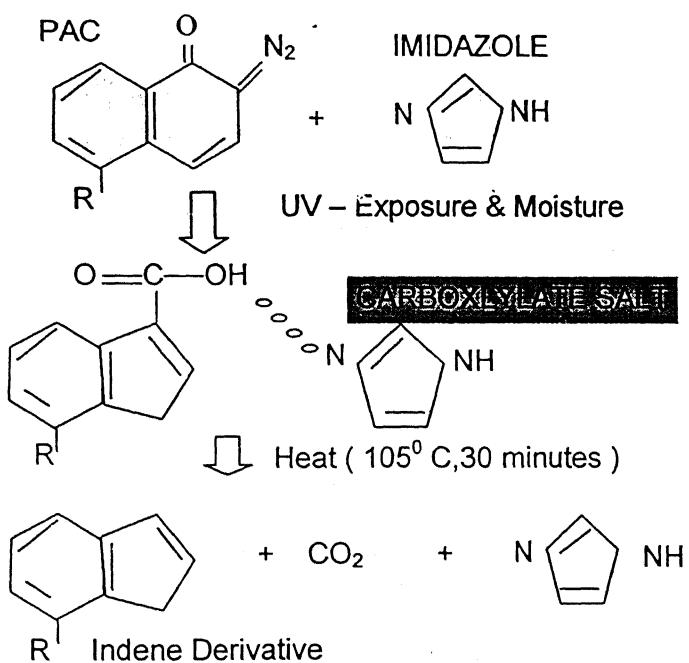
Fig 5.4: Reversal chemistry for the lift-Off process in image reversal Process

51

5.5   Process flow chart of Image Reversal:-Lift-Off Process

```
┌─────────────────────────────────────────────────────────┐
│  Adding imidizole (1% of weight) to positive photoresist  │
│     prior to spin coating atleast 30 min before           │
└─────────────────────────────────────────────────────────┘
                            ↓
┌─────────────────────────────────────────────────────────┐
│                   Cleaning Substrates                      │
└─────────────────────────────────────────────────────────┘
                            ↓
┌─────────────────────────────────────────────────────────┐
│          Dehydration Bake, $130^0$-$150^0$ C @30min        │
└─────────────────────────────────────────────────────────┘
                            ↓
┌─────────────────────────────────────────────────────────┐
│        Spin coating, 2000 rpm @ 60 Sec. (2 μm ) thick      │
└─────────────────────────────────────────────────────────┘
                            ↓
┌─────────────────────────────────────────────────────────┐
│             Soft Bake, $95^0$-$105^0$ C @30min             │
└─────────────────────────────────────────────────────────┘
                            ↓
┌─────────────────────────────────────────────────────────┐
│   * Moisture, hot water vapors ≈ $45^0$C for 15 sec        │
└─────────────────────────────────────────────────────────┘
                            ↓
┌─────────────────────────────────────────────────────────┐
│        Ultraviolet exposure(with mask) , 1-2 minutes       │
└─────────────────────────────────────────────────────────┘
                            ↓
┌─────────────────────────────────────────────────────────┐
│        ** Reversal  Bake in Oven (105°C) (30 min)          │
└─────────────────────────────────────────────────────────┘
                            ↓
┌─────────────────────────────────────────────────────────┐
│          Flood Exposure(without mask), 2-4 min,            │
└─────────────────────────────────────────────────────────┘
                            ↓
┌─────────────────────────────────────────────────────────┐
│   Develop in Shipley 312, 45:55(Developer: DI) @ 6-8 minutes │
└─────────────────────────────────────────────────────────┘
                            ↓
┌─────────────────────────────────────────────────────────┐
│                 Evaporate the metal                        │
│                         &                                  │
│           Lift-Off the Photoresist in Acetone              │
└─────────────────────────────────────────────────────────┘
```

Fig 5.5: Flow chart for the process of Lift-Off using image reversal process

* Important   ** Critical

5.6   The steps involved in the image reversal process:

(A)   Mixing of imidazole

Basic material such as imidazole or monazoline is added to the positive photoresist of 1 to 2.5 percent weight before the spin coating on the substrate. In this experiment for 13.126 grams of Photoresist 0.164 grams (i.e. of 1.25%) weight of imidazole is mixed. Imidazole takes 30 minutes to completely dissolve in photoresist. The added imidazole photoresist has got a shelf life time of 2-3 weeks. Imidazole is used to catalyze a reversal reaction (makes soluble acid to insoluble derivative) [20, 21,26].

(B)   Cleaning of substrates

The substrates (Si) are cleaned with RCA solution (1:1:5 solutions of NH_4OH, H_2O_2 and DI water). The substrates are immersed in solution and heated for 20 min., the temperature being 70^0C, followed by drying.

(C)   Photoresist coating

Spin coating with positive photoresist with a spin speed of 1500-2500 rpm for 60 seconds produces uniform layers of about 2 μm on the substrate.

(D)   Soft bake

The coated substrates were kept in the oven at a 95^0C for 30 min. for soft bake. The soft bake removes the solvent from the photoresist.

(E)   Moisture

The soft baked substrates were exposed to moisture for 15 to 60 seconds, the temperature of hot water being $45-50^0C$ followed by Ultraviolet rays (local mercury lamp) for 1-2 minutes with mask. The moisture plays a very important role in the repeatable and usable reversals [24,25].

(F) Ultraviolet Exposure

This exposure will define the actual width of the feature. The exposure transforms the photoactive compound into carboxylic acid. The imidizole molecule attaches itself to the acid forming an imidazolium carboxylate salt.

(G) Reversal Bake

The most critical parameter of the IR-process is reversal-bake temperature, once optimized it must be kept constant to ensure repeatability of the results. If IR-temperature is chosen too high (>130°C), the resist will thermally crosslink in the unexposed areas also, giving no pattern. Heating the substrates after exposure and prior to development to about 105^0C causes the salt to decay leading to release of carbon dioxide. The resultant molecule is no longer an acid; in fact it is now as poorly soluble in base developer as unexposed photoactive compound. The exposed areas are as insoluble as the unexposed areas. The exposed areas contain a light-insensitive indene derivative, while the unexposed areas still contain the original light-sensitive photoactive compound.

(H) Flood Exposure

Flood exposure or Blanket exposure (exposure with out mask) will render them soluble without altering the already exposed areas. Substrates were exposed to Ultraviolet rays (local mercury lamp) for 1-2 minutes without mask to the areas previously un-reacted, which when developed, create a negative image of the original mask with a perfect negative slop as shown in Fig 5.8(b).

The flood exposure is absolutely uncritical as long as sufficient energy is applied to make the unexposed areas soluble. By this treatment a top layer with a lowered dissolution rate compared to the bottom layer is generated.

(I)   Develop

After the flood exposure the substrates are developed for 6-8minutes in the Shipley 312 series positive photoresist developer, at room temperature with the dilution of 45:55 (Developer : DI), rinsed in DI water and dried. The development parameters would be the most critical in the reversal process. A developer that was too concentrated, would result in total removal, and a formulation too dilute would not develop. There is a possibility that more negative sidewall develops with time (negative slop increases) when developing in solution.

MASK

| I   N | I   N |
| P | P |

Substrate

After 1ˢᵗ exposure UV with Mask

| I   N | I   N |
| S | P |

Substrate

After reversal bake.

| I   N | I   N |
| U | P |

Substrate

After flood exposure without mask.

| I   N | I   N |
| U | S |

Substrate

After developing.

| I   N |
| U |

Substrate

I is the imidizole
N is the novalic
S is the soluble acid
U is the Light-insensitive derivate
    (Insoluble Derivative)
P is the Photo Active Compound

Photoresist after exposure

Photoresist

Fig. 5.6: Process sequence of Lift-Off positive photoresist
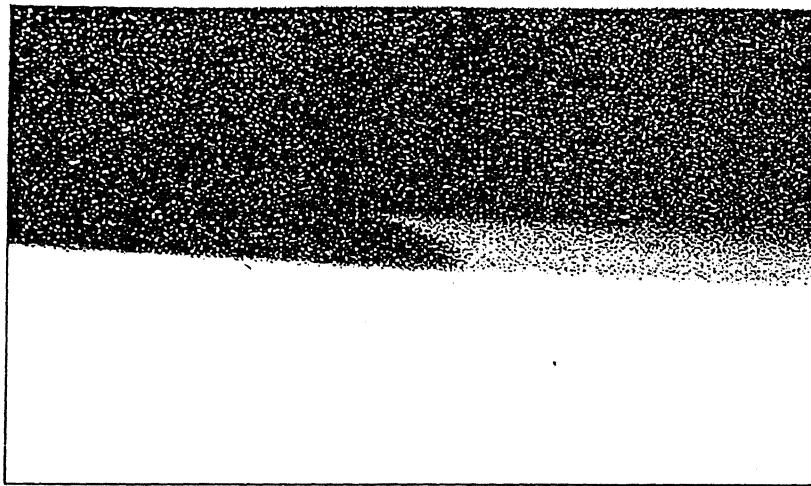
Fig 5.7: Experimental result Lift-Off: Image reversal process. (Negative slop)

Substrate is Si and Positive Photo resist is Shipley 1400 series (optical image)

(J)   Metal Evaporation

Metal evaporation is been done in the vacuum chamber with a high vacuum less than 10^{-5} mbar, melted and then evaporated. The evaporated metal will deposit on the top of the photoresist and on the substrates as shown in fig.5.10 (a) below.
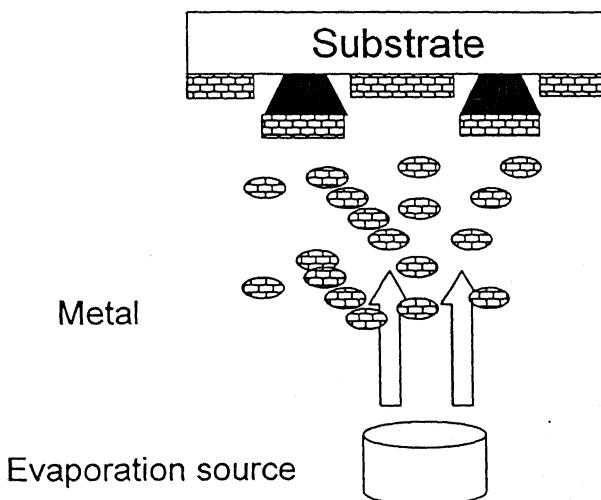
Fig 5.8(a): Metal evaporation using Lift-Off image reversal process

Metal

Photoresist

Substrate .
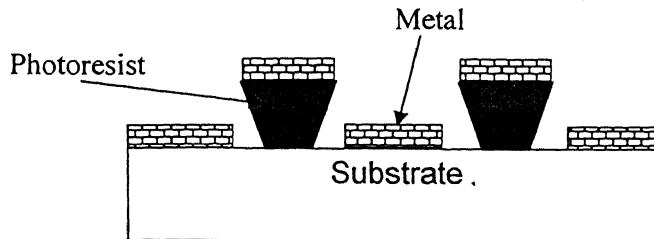
Fig 5.8(b): Metal evaporation on to the Negative sidewall

Substrate
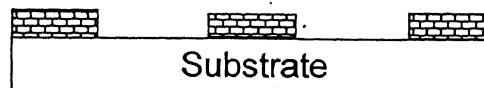
Fig 5.8(c): After Photoresist Lift-Off

After the evaporation of the material the metal deposited above the photoresist will also be lifted-off in acetone.

5.6 Advantages in organic electronics

After image reversal and metal deposition the photoresist is left outstripped in the case of organic materials. The ribs formed due to image reversal results in the necessary separation between metal lines. This procedure has two main advantages in organic electronics. First, organic materials being softer than inorganic materials won't be affected by the solvents (acetone or acids) which are normally used for stripping of photoresist. Secondly, a process step is reduced (i.e removal of PR), which results in reduction of time of processing.
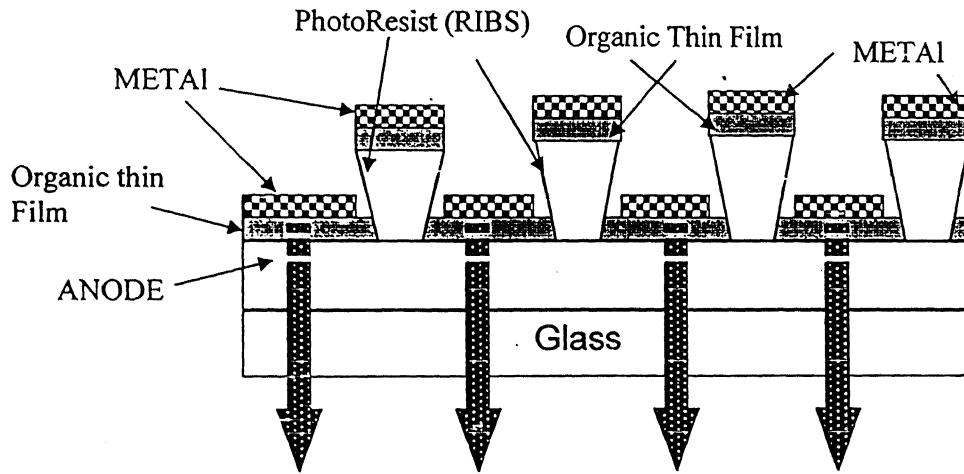
Fig 5.9: OLED/PLED the rib like structure is done with IR process prior to the polymer deposition.

Photolithography is done prior to the deposition of the Organic/polymer film and cathode [30], high resolution is possible leading to large area thin film applications. The organic materials are inherently susceptible to damage from organic solvents which are generally used to remove photoresist (like acetone). Therefore, it is better if the photoresist is not removed.

In this image reversal process, the photoresist can be left as such thereby avoiding a wet process step ultimately leading to saving of time and avoiding damage to the active material. The desired resist structure must be taller than the thickness of the metal to be evaporated in order to eliminate bridging of the metal on the substrate to the metal on top of the resist. The structure should have a small overhang (the top of the resist line larger than the bottom) so that the metal is not evaporated on the sidewalls of the photoresist, and yet the overhang should be large enough to ensure consistent isolation.

5.8   FUTURE WORK

SOFT LITHOGRAPHY

Unlike most polymers, conducting polymers have the electrical and optical properties of metals or semiconductors. These materials are of increasing interest in microelectronics because they are inexpensive, flexible and easy to synthesize.

Some of the conducting polymers have the nature of non-conducting when exposed to Ultra violet rays. Thus have the advantage of control over critical temperature in the Lift-Off process which ultimately reduces the fabrication process, cost and time. D. M. de Leeuw, C. M. J. Mutsaers, and M. M. J. Simenon, have demonstrated this model in all polymer ICs[28]. Such as Polyaniline doped with camphorsulfonic acid is dissolved in *m*-cresol.
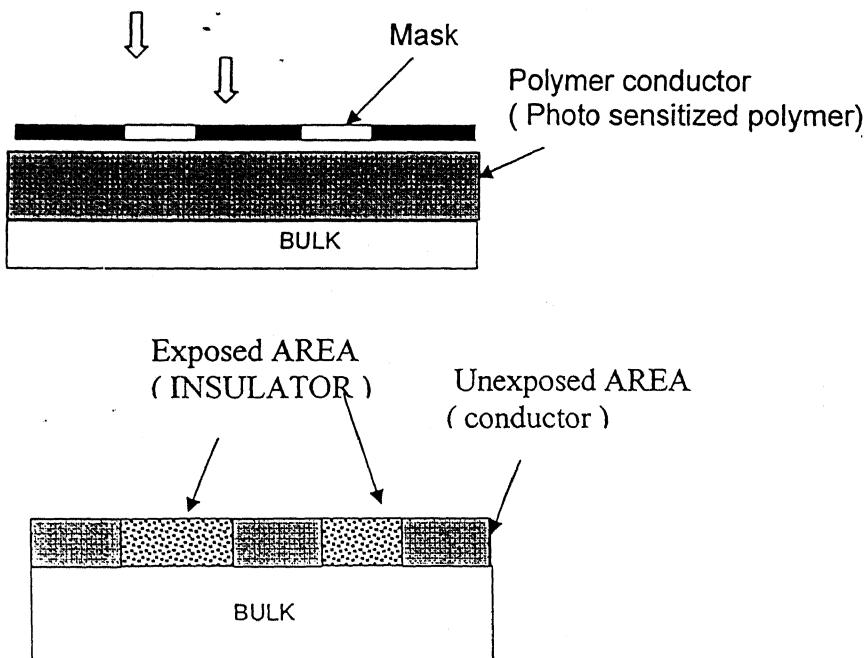
Fig 5.10: Soft lithography of Patterning of metal polymer

A photo initiator, is added to this solution which is then spin-coated onto a substrate (such as polyimide foil). Under an inert atmosphere the film is exposed through a mask to deep ultraviolet (UV) radiation. Upon exposure the conducting

polyaniline is reduced to the no conducting leucoemeraldine form. The conducting PANI tracks are used as interconnects and as electrodes [26,27,28].

5.9   Summary:

Lift-off is excellent technique for the reproducibility of the patterning the thinner metals, as it needs no etching offers cost and density advantage. The first exposure has a strong effect on the negative sidewall profile and also determines the line widths. The moisture and the reversal bake are the only critical parameters involved in this process, can be overcome by the process optimization. The size of mask does not matter, hence used for the displays and VLSI area where the resolution matters. Soft lithography will be the budding technique, and become popular very soon as if we get a conducting polymer of N-type which will be capable of separating isolation when expose to UV.

CONCLUSSION and FUTURE WORK

The nature of the hole current is space charge limited for the all thickness of PEDOT and it is also independent of PEDOT layer thickness. But only with 850 A^0 the yield is high, so in order to have high yield we have to use $850A^0$ PEDOT only because the surface roughness changes from ITO-MEH-PPV interface to PEDOT-MEH-PPV interface.

The electron current is a strong function of Ca layer thickness and reaches the SCLC value at a Ca layer thickness of $200A^0$. Beyond a certain value of electric field for thicker Ca, the effective barrier for electron is lowered and the FN-tunneling mechanism is activated leading to current values larger than SCLC.

By finding the nature of electron current and hole current separately by fabricating hole-only and electron-only devices, then appropriate contact conditions at anode and cathode respectively have been found out to ensure maximum (i.e. SCLC) injection of both holes and electrons can be used. This information can be used to make a PLED which has better luminescence and optimal efficiency.

Experiments can be designed to ensure charge balance which will lead to maximum efficiency.

Lift-Off:-Image reversal process in a positive photoresit is used for the cathode isolation of OLEDs/PLEDs in a displays applications etc., where the utility of ribs like photoresist is required.

Derivation for Space Charge Limited Current

Both FN tunneling and Poole-Frenkel emission mechanism yield very low current densities with correspondingly low carrier densities. For structures where carriers can readily enter the insulator and freely flow through the insulator one finds that the resulting current and carrier densities are much higher. The density of free carrier causes a field gradient, which limits the current density. This situation occurs in lowly doped semiconductors and vacuum tubes. In organic polymers, there are no charge carriers. Therefore the current will be only due to drift. Starting from an expression for the drift current and Gauss's law where we assume that the insulator contains no free carriers if no current flows.

$$J = q \, p \, \mu \, \varepsilon \qquad\qquad (A1)$$

$$\frac{d\varepsilon}{dx} = \frac{q\,p}{\varepsilon} \qquad\qquad (A2)$$

We can eliminate the carrier density, p, yielding:

$$\frac{J}{\varepsilon\,\mu} = \varepsilon \, \frac{d\varepsilon}{dx} \qquad\qquad (A3)$$

Integrating this expression from 0 to x, where w assume the electric field to be zero at $x = 0$ one can obtains:

$$\frac{Jx}{\varepsilon\mu} = \varepsilon^2 \quad or \quad \varepsilon(x) = \sqrt{\frac{2xJ}{\varepsilon\mu}} \qquad (A4)$$

Integrating once again from $x = 0$ to $x = d$ with V (0) = V and V (d) = 0,

$$V = \int_0^d \varepsilon \, dx = \sqrt{\frac{2\,J}{\varepsilon\mu}} \frac{d^{3/2}}{3/2} \qquad (A5)$$

From which one obtains the expression for the space-charge-limited current:

$$J = \frac{9\,\varepsilon\,\mu\,V^2}{8\,d^3} \qquad (A6)$$

CHARACTERISATION OF ORGANIC LIGHT EMITTING DIODE

Measuring the current and voltage in a Organic light emitting diodes is usually done by oscilloscope, but data cannot be saved. Using Source Measure Unit (SMU) it is easier to measure these characteristics. Normaliy SMU has IEEE commands to use for computer interface. These characteristics can be measured by software HP 4.00 and Labview and data can be saved.
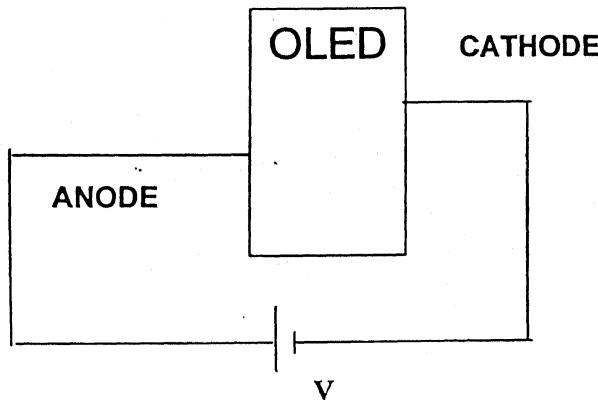

Figure B-1. OLED/PLED with an applied voltage to anode and cathode

OLED or organic light emitting diode is currently one of the major research areas for various applications like displays etc. Since these are made of organic materials they are cheap and consume less power.

BLOCK DIAGRAM

```
                    ┌──────────────────────┐
                    │        GPIB          │
                    └──────────────────────┘
┌─────────────────┐  ┌──────────────────────┐        ┌─────────────────┐
│ KETHLY 193      │  │ KEITHLY 236\237      │        │                 │
│ SYSTEM          │  │ (Source Measure Unit)│  GPIB  │  CPU With DAQ   │
│ DMM             │  │                      │        │                 │
│ (Measure  unit  │  └──────────────────────┘        └─────────────────┘
│ Voltage)        │              ↕
├─────────────────┤  ┌──────────────────────┐        ┌─────────────────┐
│ Si Photo Detector│  │     DEVICE            │       │    MONITER      │
│                 │←─│   UNDER TEST          │        │                 │
└─────────────────┘  └──────────────────────┘        └─────────────────┘
```
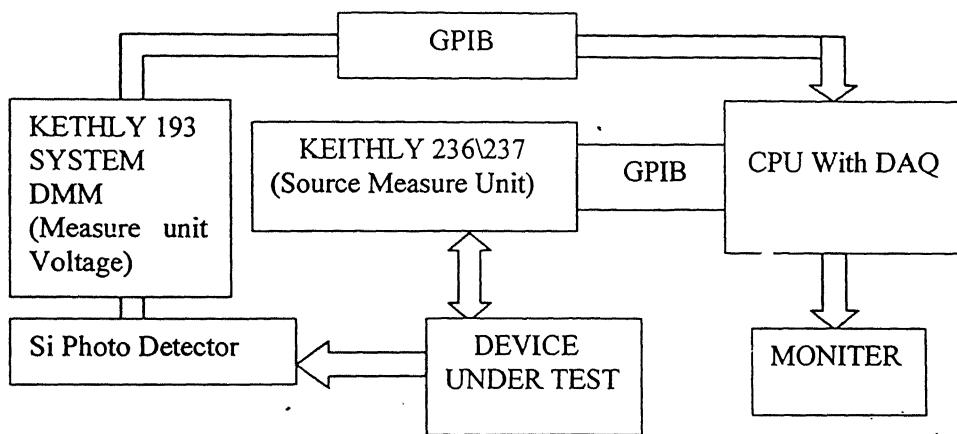
Figure B-2: Block diagram for the characterization of OLED Using GPIB cables (IEEE)

The Device under Test (DUT) is connected with a pair of connectors with Keithly (SMU) source measure unit, in order to source voltage, current and measure voltage current. SMU supplies Voltage and measures Current. A Fiber optic cable is connected to DUT to measure the photo current.

Photo detector is a sensor (transducer) measures light and supplies current, a resistor across this current gives a voltage which is measured by Keithly 193 DMM. This further can be converted to current of the photo detector.

This data is written to CPU with the help of General-Purpose Interface Bus (GPIB).
Like J0x - restores to factory default conditions, etc. all the commands given below.

SMU supplies voltage with a rage of 0-3v (our case) with a step of 0.1volts linear stair case sweep. And data is available in terms of string. This data is read by GPIB by

SRQ.i.e (M Command). This string is converted by string subset and fowled by substring to differentiate Voltage and Current of the device.

Similarly for photo current. The Photo detector is activated by some DC supply measures the Number of photons and converted into current. This current flows through a resistor which gives a measure of voltage.

Characteristics of OLED:

1)   Applied Voltage VS   OLED Current
2)   Photo current   VS   Applied Voltage
3)   Photo current   VS   OLED Current

IEEE 488 COMMANDS USED FOR KETHLY (SMU):

Source Measure unit commands

IEEE 488 Bus address   18 (00 to 30)

J0x - restores to factory default conditions

F0, 1X   - Sources V measures I

        0, 0 sources V and measures I, (DC)

        0, 1 sources V and measures I,(Sweep)

        1, 0 source I and measures V, (DC)

        1, 1 sources I and measures V,(Sweep)

0 0x Select local sense

01 x select remote sense

L40e-03,0x

       0 => auto

       40e-03 => compliance; max val of I (current)

G5, 2,1x, G, items, format, lines

       5=> send both v and i

       2=> ASCII data, no prefix or suffix.

       1=> one line of sweeps data per talk

Selects the type format and duty of o/p data transmitted over the bus.

=> Use ASCII format and transmit both the V and I

M2, x

       M (mask), compliance

       2=>Sweep is done

       All data taken is available for reading

T1, 0, 0, 0

       T (origin), in, out, sweepend

       T1=> Trigger on

       0=> cont. input; 0=>nothing for o/p; 0=> end is disabled

S3

       To control the integration time 20ms for our case.

B0,0,0

       B lvl, range, delay; lvcl=> i or v; range=>auto; delay=none ; To programe

       the dc bias operation , the non trigger sweep src value and the T off src value of

       pulse sweep

Q1,0.0,3.0,0.1,0,500

       Q,start,stop, step,range,delay

       0=>auto range

R1N1

       To enable or disable i/p and o/p trigger

       R1 start trigger.

       N1 start immediately if 0 then stand by

H0x

       Immediate bus trigger. To provide and immediate trigger stimulus for the **IEEE** bus.

Photo Detector system commands

IEEE 488 Bus address   10

F0   change to DC function

R0   disable i/p trigger and generate of o/p trigger

S3   integration time

LABVIEW---Block Diagram.
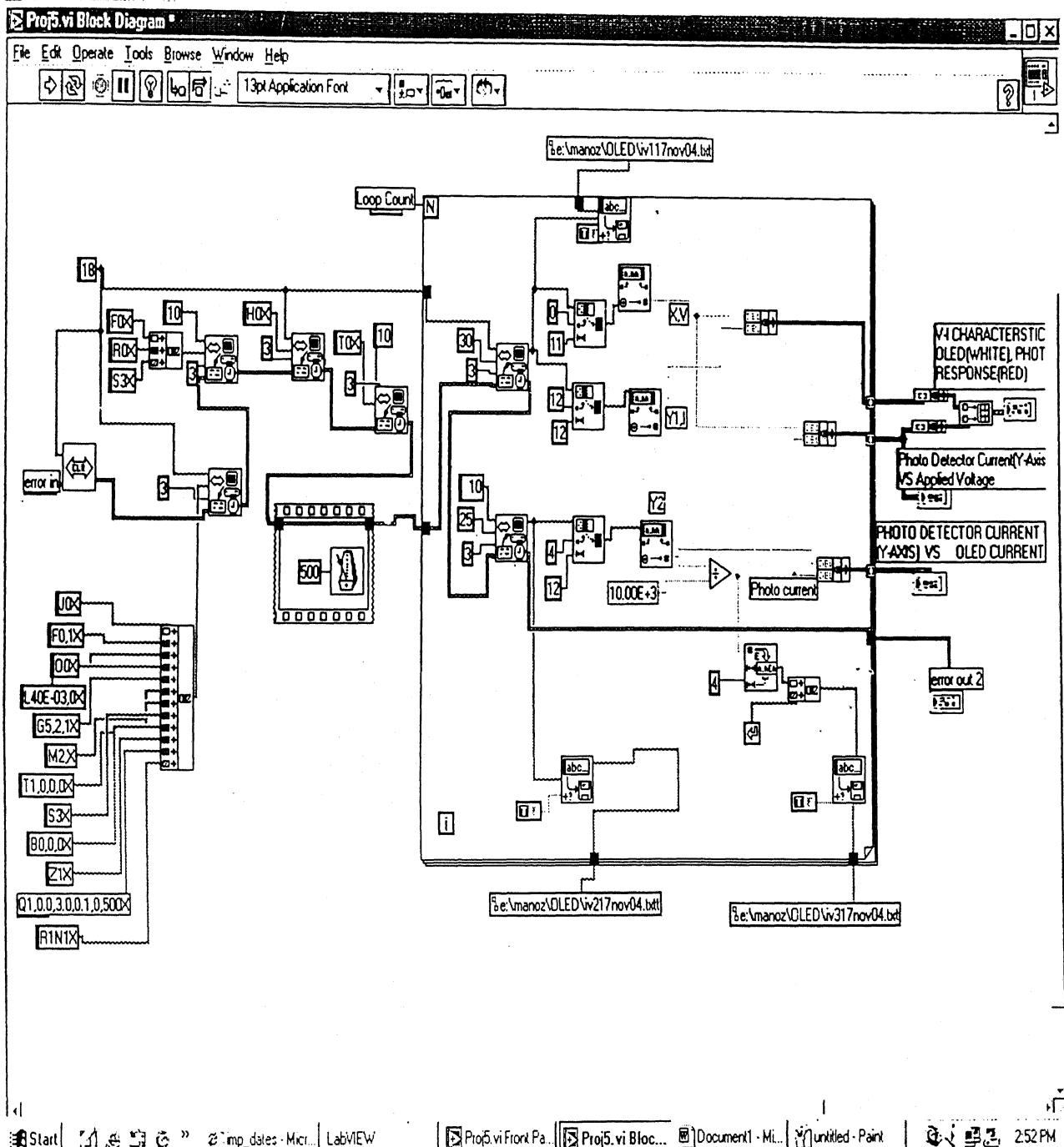
Figure B-3: Block diagram for the characterization of OLED in LabView 7.1

LABVIEW---FRONT PANEL Diagram
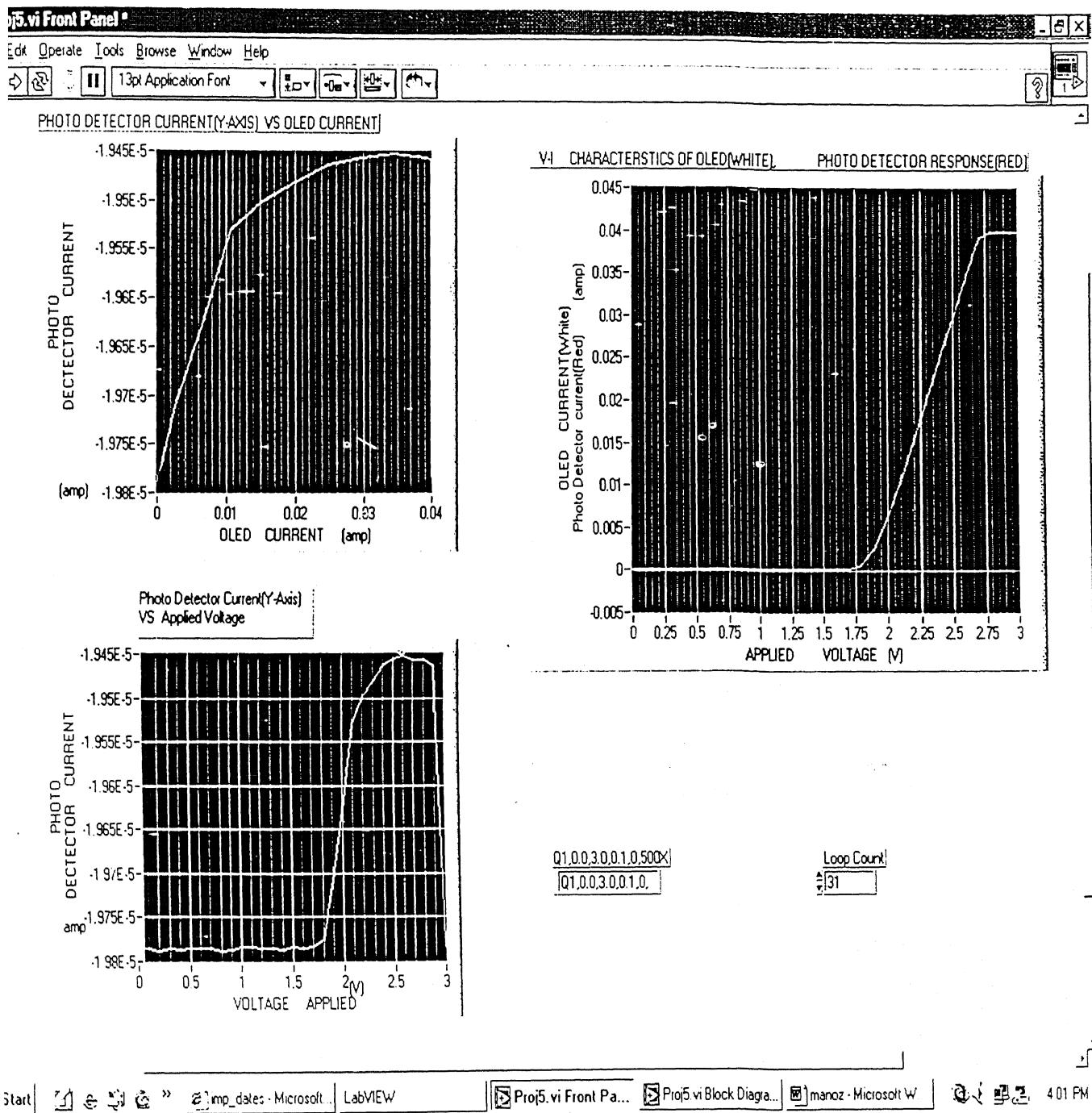
Figure B-4: Front Panel of the characterization of OLED Using LabView 7.1

References

[1]   Pope and Swenberg, *"Electronic processes in organic crystals"* Clarendon press,Oxford, 1982

[2]   C.W.Tang and S.A.Vanslyke, *"Organic electroluminescent diodes"*, Applied Physics Letters vol. 51, no.12, pages- 913-915, September 1987

[3]   A.R. Brown, D.D.C. Bradley, P.L. Burns, J.H. Burroughes, R.H. Friend, N. Greenham, A.B. Holmes, A. Kraft, *"Poly(p-phenylenevinylene) light-emitting diodes: Enhanced electroluminescent efficiency through charge carrier confinement"*, Applied Physics Letters vol. 61, no. 23, pages- 2793-2795,December 1992

[4]   I.D.Parkar, *"Carrier tunneling and deice characteristics in polymer light emitting diodes"*, J.Appl.Physics vol.75, no.3, pages- 1656-1666, February 1994.

[5]   L.Bozano, S.A. Carter, J.C.Scott, G.G.Milliaras, *"Temperature-and Field-dependent electron and hole mobilities in Polymer- light emitting diodes"*, Applied Physics Letters, vol.74, no.8, pages-1132-1135, February 1999

[6]   V.I.Arkhipova, H.von Seggern, E.V.Emelianova, *"Charge injection versus space-charge-limited current in organic light emitting diodes"* Applied physics letters, vol.83, no.24, pages- 5074-5076, December 2003

[7]   S. A. Carter, M. Angelopoulos, S. Karg, P. J. Brock, and J. C. Scott, *"Polymeric anodes for improved PLED performance"*, Applied Physics Letters, vol.70 no.16, pages- 2067-2069, April 1997

[8]   D.B.A. Rep, A.F.Morpurgo, T.M.Klapwijk, *"Doping-dependent charge injection into regioregular poly(3-hexylthiophene)"*, Organic Electronics, vol.4, pages- 201-207, 2003

[9]   J.M.Houston, *"The slope of logarithmic plots of the Fowler-Nordheim equation"*, Physics Review, vol.88, no.2, pages-346, 1952

[10]   Daisuke Moritaa, Masahiko Kitagawaa, Hiroyuki Kusano, Shinji Kawakami, Toshihiko Tsushima, Tatsuhiro Sawada , Kazuaki Hatano, Yasuo Hirooka, Hiroshi Kohayashi, *"Charg transport in PVCz EL using multi-layered PVCz film doped with Cz"*, Synthetic metals, 111-112, pages-217-220, 2000

[11]   Herbert B. Michaelson, *"The work function of the elements and its periodicity"*, Journal of applied Phuysics., vol. 48, no. 11, pages- 4729-4732, November 1977

[12]   D.P.Halliday, J.M.Eggleston, P.N.Adams,   I.A.Pentland and A.P.Monkman, *"Vishle   Electroluminescence   from   a   Polyaniline-Porous   Silicon junction"*,Synthetic Metals vol.85, pages-1245-1246, 1997

[13]   J.Narain, J.M.Borregg, R.J.Gutmann *"Effect of chromium thickness on Au Cr-nSi schottky and Au Cr-n-P Si baritt diodes"*, Electron Letters, vol.11, no.8, pages-178-179, April 1975

[14]   S. A. Carter, M. Angelopoulos, S. Karg, P. J. Brock, and J. C. Scott, *"Polymeric anodes for improved PLED performance"*, Applied Physics Letters, vol.70 no.16, pages- 2067-2069, April 1997

[15]   D.B.A. Rep, A.F.Morpurgo, T.M.Klapwijk, *"Doping-dependent charge injection into regioregular poly(3-hexylthiophene)"*, Organic Electronics, vol.4, pages-201-207, 2003

[16]   Herbert B. Michaelson, *"The work function of the elements and its periodicity"*, Journal of applied Phuysics., vol. 48, no. 11, pages- 4729-4732, November 1977

[17]   D.P.Halliday, J.M.Eggleston, P.N.Adams,   I.A.Pentland and A.P.Monkman, *"Visible Electroluminescence from a Polyaniline-Porous Silicon junction"*, Synthetic Metals vol.85, pages-1245-1246, 1997

[18]   D.P.Halliday, T.A.Coulter, J.W.Gray, P.N.Adams, *"Visible electroluminescence from a polymer semiconductor junction"*, Proceedings of the 24th International Conference on the Physics of Semiconductors, Jerusalem, Israel, 2 – 7, pages- 1-4, August 1998.

[19]   Holger Moritz, *"Optical single layer lift-off process"*, IEEE Transactions on Electron Devices vol.32, no.3, pages- 672-676, March 1985.

[20]   M. Hatzakis, B. J. Canavello, and J. M. Shaw, *"Single-Step Optical Lift-off Process"*, IBM Journal of Research and Development, vol.24, no.4, pages-452-460, July 1980

[21]   George G. Collins, and Cary W. Halsted, *"Process Control of the Chlorobenzene Single-Step Liftoff Process with a Diazo-Type Resist"*, IBM Journal of Research and Development, vol.26 no.5, pages-596-604, September 1982

[22]   Caryn Hartglass, *"Optimization of image reversal of positive photoresist"*, Ultratech Photomask, Santa Clara, California, pages-1-10

[23]   Image reversal resist system AR-U 4000, pages-1-10, January 2003

[24]   S. A. Carter, M. Angelopoulos, S. Karg, P. J. Brock, and J. C. Scott, *"Polymeric anodes for improved PLED performance"*, Applied Physics Letters vol.70 no.16, pages- 2067-2069, April 1997

[25]   G. H. Gelinck, T. C. T. Geuns, and D. M. de Leeuw , *"High-performance all-polymer integrated circuits"*, Applied Physics Letters vol.77, no.10, pages- 1487-1489, September 2000

[26]   C. J. Drury, C. M. J. Mutsaers, C. M. Hart, M. Matters, and D. M. de Leeuw, *"Low-cost all-polymer integrated circuits"*, Applied Physics Letters, vol.73, no.1, pages-108-110, July 1998

[27]   Graciela B. Blanchet, DuPont, Yueh-Lin Loob and J. A. Rogers F. Gao and C. R. Fincher, *"Large area, high resolution, dry printing of conducting polymers for organic electronics"*, Applied Physics Letters vol.82, no.3, pages- 463-465, January 2003

[28]   Frey, D. W., Guild, J.R., and Hryhorenko, E.B., *"Edge Profile and Dimensional Control for Positive Photoresist"*, Interface'81, Dallas, Texas, 1981.

[29]   Daniel B.Roitman, Homer Antoniadis, Rene Helbing, Fereidoun Pourmizaie, James R. Sheats *"Polymer Light emitting Devices Based on POlyfluorenes"* part of the SPICE Conference on Organic Light-Emitting materials and Devices-IId, San Diego, California, pages-232-241, july 1998

[30]   Degao Xu, Gerald D. Watt, John N.Harb, and Robert C.Davis, *"Electrical conductivity of Ferritin Proteins by Conductive AFM"*, Nano Letters, XXXX, vol.0, No.0, A-G

[31]   J.Maserjian and N.Zamani, *"Behavior of the Si/SiO$_2$ interface observed by Fowler-Nordheim tunneling"*, J.Appl.Phys, vol.53, no.1, pages-559-567, January 1982

[32]   V Kazukauskas, *"Investigation of carrier transport and trapping by oxygen-related defects in MEH-PPV diodes"*, Semicond Sci. Technol, vol.19, pages-1373-1380, 2004

[33]   Mary L. Long, Jeff Newman, *"Image reversal techniques with standard positive photoresist"*, KTI Chemicals, Inc., 4040 N, & Electrical and Computer Engineering, College of Engineering University of Arizona, Tucson, AZ. 85721